

## Module 7 : Lecture 1

### MEASUREMENTS IN FLUID MECHANICS

#### (Incompressible Flow – Part I)

#### Overview

Accurate measurement in a flowing medium is always desired in many applications. The basic approach of the given measurement technique depends on the flowing medium (liquid/gas), nature of the flow (laminar/turbulent) and steady/unsteadiness of the medium. Accordingly, the *fluid flow diagnostics* are classified as measurement of *local properties* (velocity, pressure, temperature, density, viscosity, turbulent intensity etc.), *integrated properties* (mass and volume flow rate) and *global properties* (flow visualization). Also, these properties can be measured directly using certain devices or can be inferred from few basic measurements. For instance, if one wishes to measure the flow rate, then a direct measurement of volume/mass flow can be done during a fixed time interval. However, the secondary approach is to measure some other quantity such as pressure difference and/or fluid velocity at a point in the flow and then calculate the flow rate using suitable expressions. In addition, flow-visualization techniques are sometimes employed to obtain an image of the overall flow field. The *parameters of interest for incompressible flow* are the fluid viscosity, pressure/temperature, fluid velocity and its flow rate.

#### Measurement of Viscosity

The device used for measurement of viscosity is known as *viscometer* and it uses the basic laws of laminar flow. The principles of measurement of some commonly used viscometers are discussed here;

Rotating Cylinder Viscometer: It consists of two co-axial cylinders suspended co-axially as shown in the Fig. 7.1.1. The narrow annular space between the cylinders is filled with a liquid for which the viscosity needs to be measured. The outer cylinder has the provision to rotate while the inner cylinder is a fixed one and has the provision to measure the torque and angular rotation. When the outer cylinder rotates, the torque is transmitted to the inner stationary member through the thin liquid film formed between the cylinders. Let  $r_1$  and  $r_2$  be the radii of inner and outer cylinders,  $h$  be the depth of immersion in the inner cylinder in the liquid and  $t (= r_2 - r_1)$  is the annular

gap between the cylinders. Considering  $N$  as the speed of rotation of the cylinder in rpm, one can write the expression of shear stress ( $\tau$ ) from the definition of viscosity ( $\mu$ ), as given below;

$$\tau = \mu \frac{du}{dy} = \mu \left( \frac{2\pi r_2 N}{60t} \right) \quad (7.1.1)$$

This shear stress induces viscous drag in the liquid that can be calculated by measuring the torque through the mechanism provided in the inner cylinder.

$$T = \text{shear stress} \times \text{area} \times \text{radius} = \mu \left( \frac{2\pi r_2 N}{60t} \right) (2\pi r_1 h) r_1 \quad (7.1.2)$$

$$\text{or, } \mu = \frac{15tT}{\pi^2 r_1^2 r_2 h N} = \frac{T}{CN}$$

Here,  $C$  is a constant quantity for a given viscometer.

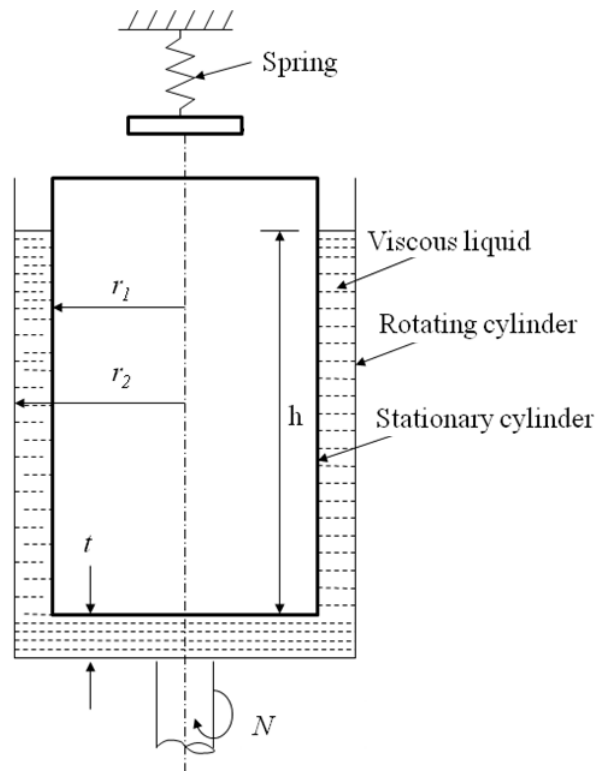


Fig. 7.1.1: Schematic nomenclature of a rotating cylinder viscometer.

**Falling Sphere Viscometer:** It consists of a long container of constant area filled with a liquid whose viscosity has to be measured. Since the viscosity depends strongly with the temperature, so this container is kept in a constant temperature bath as shown in Fig. 7.1.2.

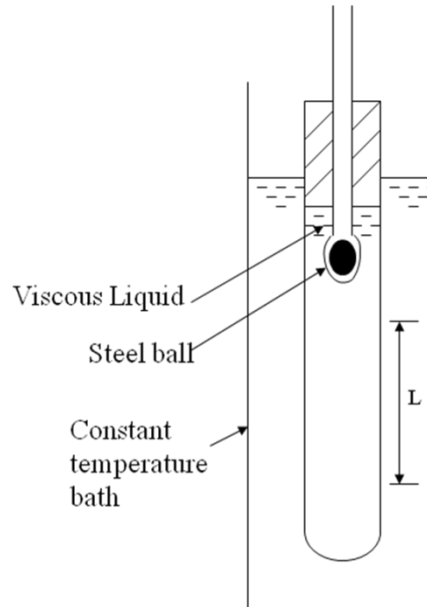


Fig. 7.1.2: Schematic diagram of a falling sphere viscometer.

A perfectly smooth spherical ball is allowed to fall vertically through the liquid by virtue of its own weight ( $W$ ). The ball will accelerate inside the liquid, until the net downward force is zero i.e. the submerged weight of the ball ( $F_B$ ) is equal to the resisting force ( $F_R$ ) given by *Stokes' law*. After this point, the ball will move at steady velocity which is known as *terminal velocity*. The equation of motion may be written as below;

$$F_B + F_R = W \quad \Rightarrow \quad \frac{\pi}{6} D^3 w_l + F_R = \frac{\pi}{6} D^3 w_s \quad (7.1.3)$$

where,  $w_l$  and  $w_s$  are the specific weights of the liquid and the ball, respectively. If the spherical ball has the diameter  $D$  that moves at constant fall velocity  $V$  in a fluid having viscosity  $\mu$ , then using Stokes' law, one can write the expression for resisting force ( $F_R$ ).

$$F_R = 3\pi \mu V D \quad (7.1.4)$$

Substituting Eq. (7.1.4) in Eq. (7.1.3) and solving for  $\mu$ ,

$$\mu = \frac{D^2}{18V} (w_s - w_l) \quad \text{where } V = \frac{L}{t} \quad (7.1.5)$$

The constant fall velocity can be calculated by measuring the time ( $t$ ) taken by the ball to fall through a distance ( $L$ ). It should be noted here that the falling sphere viscometer is applicable for the Reynolds number below 0.1 so that wall will not have any effect on the fall velocity.

**Capillary Tube Viscometer:** This type of viscometer is based on laminar flow through a circular pipe. It has a circular tube attached horizontally to a vessel filled with a liquid whose viscosity has to be measured. Suitable head ( $h_f$ ) is provided to the liquid so that it can flow freely through the capillary tube of certain length ( $L$ ) into a collection tank as shown in Fig. 7.1.3. The flow rate ( $Q$ ) of the liquid having specific weight  $w_l$  can be measured through the volume flow rate in the tank. The *Hagen-Poiseuille* equation for laminar flow can be applied to calculate the viscosity ( $\mu$ ) of the liquid.

$$\mu = \left( \frac{\pi}{128} \right) \frac{w_l h_f d^4}{QL} \quad (7.1.6)$$

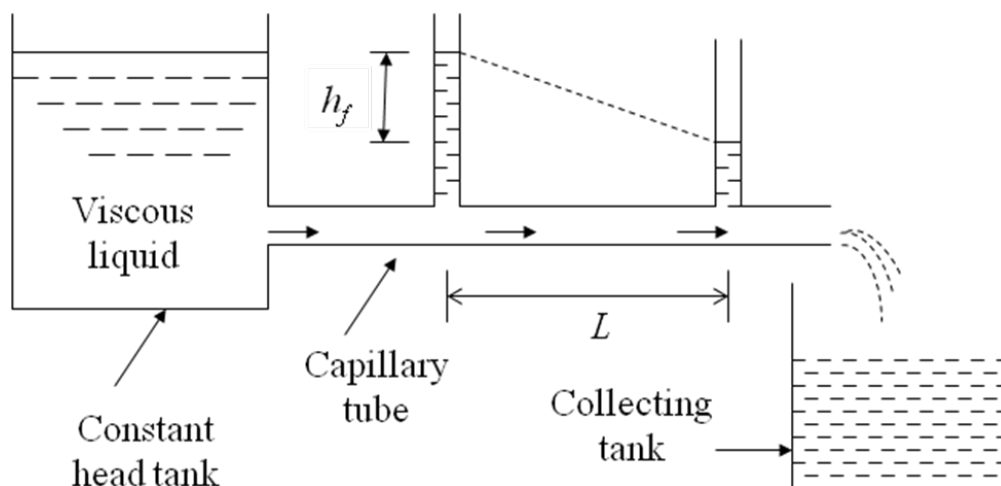


Fig. 7.1.3: Schematic diagram of a capillary tube viscometer.

Saybolt and Redwood Viscometer: The main disadvantage of the capillary tube viscometer is the errors that arise due to the variation in the head loss and other parameters. However, the *Hagen-Poiseuille* formula can be still applied by designing a efflux type viscometer that works on the principle of vertical gravity flow of a viscous liquid through a capillary tube. The *Saybolt viscometer* has a vertical cylindrical chamber filled with liquid whose viscosity is to be measured (Fig. 7.1.4-a). It is surrounded by a constant temperature bath and a capillary tube (length 12mm and diameter 1.75mm) is attached vertically at the bottom of the chamber. For measurement of viscosity, the stopper at the bottom of the tube is removed and time for 60ml of liquid to flow is noted which is named as *Saybolt seconds*. So, Eq. (7.1.6) can be used for the flow rate ( $Q$ ) is calculated by recording the time (*Saybolt seconds*) for collection of 60ml of liquid in the measuring flask. For calculation purpose of kinematic viscosity ( $\nu$ ), the simplified expression is obtained as below;

$$\nu = \frac{\mu}{\rho} = 0.002t - \frac{1.8}{t}; \text{ where, } \nu \text{ in Stokes and } t \text{ in seconds} \quad (7.1.6)$$

A *Redwood viscometer* is another efflux type viscometer (Fig. 7.1.4-b) that works on the same principle of *Saybolt viscometer*. Here, the stopper is replaced with an orifice and *Redwood seconds* is defined for collection of 50ml of liquid to flow out of orifice. Similar expressions can be written for *Redwood viscometer*. In general, both the viscometers are used to compare the viscosities of different liquid. So, the value of viscosity of the liquid may be obtained by comparison with value of time for the liquid of known viscosity.

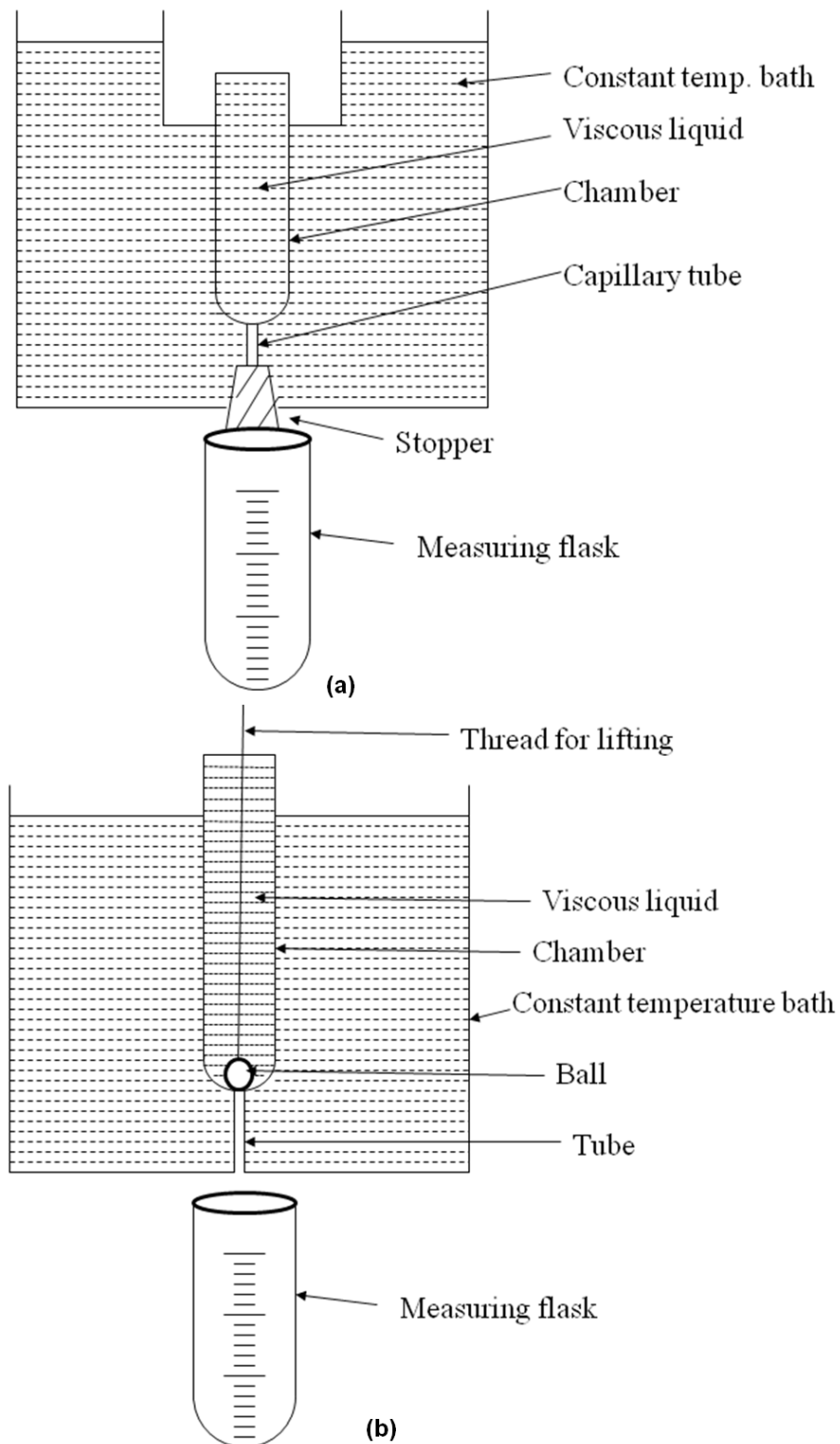


Fig. 7.1.4: Schematic diagram: (a) Saybolt viscometer; (b) Redwood viscometer.

## Measurement of Pressure

The fluid pressure is usually measured with reference to standard atmosphere (i.e. 760mm of mercury/101.325 kPa). Any differential pressures are often expressed as *gauge/vacuum* pressure. The pressure measuring devices mostly employed in fluid systems are generally grouped under two categories; *liquid manometers and mechanical gauges*.

The liquid manometers work on the principle of balancing the column of liquid whose pressure is to be determined by same/another liquid column. Depending on the application, magnitude of pressure and sensitivity requirement, the manometers can be selected. The most commonly used liquid as manometric fluid are mercury, water, alcohol and kerosenes etc. Most of the case, for gauge pressure measurements, mercury is widely used as manometric fluid because it has non-evaporating quality under normal conditions, sharp meniscus and stable density. For some pressure differences and low level vacuum, water can be considered as working fluid in the manometer. Manometers can be employed to measure pressures in the range of 0.4 Pa to 200 kPa.

The liquid manometers become bulky for handling higher pressure measurements. In such cases, mechanical gauges are normally employed. These gauges employ elastic elements which can deflect due to pressure acting on it. The deflection obtained by action of pressure is mechanically magnified and made to operate a pointer moving in a graduated dial. Some of these mechanical devices are dead-weight pressure gauges, bourdon tube pressure gauge, elastic diaphragm pressure gauges, pirani and McLeod gauges (vacuum measurement) etc.

## Measurement of Temperature

Temperature is a thermodynamic property of a fluid which is measured as a change with respect to another temperature-dependent property. In practical aspects, the temperature is gauged by its effect on quantities such as volume, pressure, electrical resistance and radiant energy. The temperature sensing devices working on these techniques are classified in the following categories;

- Thermometers (changes in physical dimension and gas/vapour pressures)
- Resistance temperature detectors (RTD), Thermistors, Thermocouples, Semiconductor sensors (changes in electrical properties)

- Pyrometers (Changes in thermal radiation)

Among all the devices, the electrical temperature sensors are mostly used particularly when automatic/remote recording is desired. Radiant sensors are used for noncontact temperature sensing, either in high temperature applications (combustors) or for infrared sensing at low temperatures. These are optical devices and can be adapted to whole-field temperature measurements known as thermal imaging. The most familiar type of temperature sensing device is the thermometer that appears in laboratories and households because of its ease in use and low cost. Some of the important and commonly used temperature devices are discussed here.

Resistance Thermometers and Thermistors: Traditionally, the resistance elements sensitive to temperatures are made out of metals which are good conductors of electricity (e.g. nickel, platinum, copper and silver). The operating ranges for this class of devices fall between – 250°C to 1000°C. They are commonly referred as resistance temperature detectors (RTD) and provide a linear temperature-resistance relation.

$$\frac{R}{R_0} = 1 + \alpha_c (T - T_0) \quad (7.1.7)$$

Here,  $R$  is the resistance at temperature  $T$ ,  $R_0$  is the resistance at reference temperature  $T_0$  and  $\alpha_c$  is the temperature coefficient of resistance depending on the material (Fig. 7.1.5)



There are certain classes of semiconducting materials (such as metal oxides of cobalt, manganese and nickels) having negative coefficient of resistances. These devices are called as *thermistors* for which the resistance temperature relation is non-linear as given below;

$$\frac{R}{R_0} = \exp \left[ \beta_t \left( \frac{1}{T} - \frac{1}{T_0} \right) \right] \quad (7.1.7)$$

where,  $\beta_t$  is a constant for a given *thermistor*. The practical operating ranges for the thermistor lie approximately between  $-100^\circ\text{C}$  to  $275^\circ\text{C}$ .

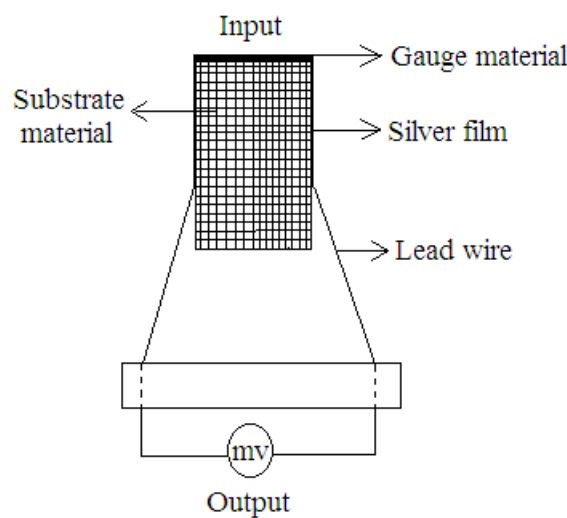


Fig. 7.1.5: Representation of a resistance temperature gauge.

**Thermocouples:** When two dissimilar metals are joined together to form a junction, then an electromotive force exists between the junctions and the connecting wires that forms the circuit. It leads to a current flow in the circuit due to the potential difference of voltage that comes from two different sources: from contact of two dissimilar metals at the junction temperature and from the temperature gradients along the conductors in the circuit. The first one is known as *Peltier effect* which is due to the temperature difference between the junctions. The voltage difference due to temperature gradients along the conductors in the circuit is known as *Thomson effect*. In most of the cases, the Thomson emf is quite small relative to *Peltier emf* and with proper selection of conductor materials, the *Thomson emf* can be neglected. With this principle, a thermocouple is prepared between two conductors of different materials resulting two junctions *p* and *q* as shown in Fig. 7.1.6. If the junction temperatures

( $T_1$  and  $T_2$ ) are equal, then the emfs will balance and no current will flow. When there is temperature difference between the junctions, then there will be net emf and a current will flow in the circuit. When the thermocouple is used to measure an unknown temperature, then temperature of one of the junctions is known and termed as *reference junction* and by measuring the net emf in the circuit, the unknown temperature can be measured. The thermocouple circuits also follow certain laws in addition to Seebeck effect;

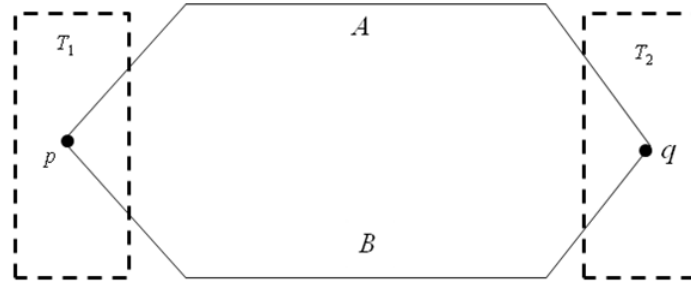


Fig. 7.1.6: Schematic representation of a thermocouple junction.

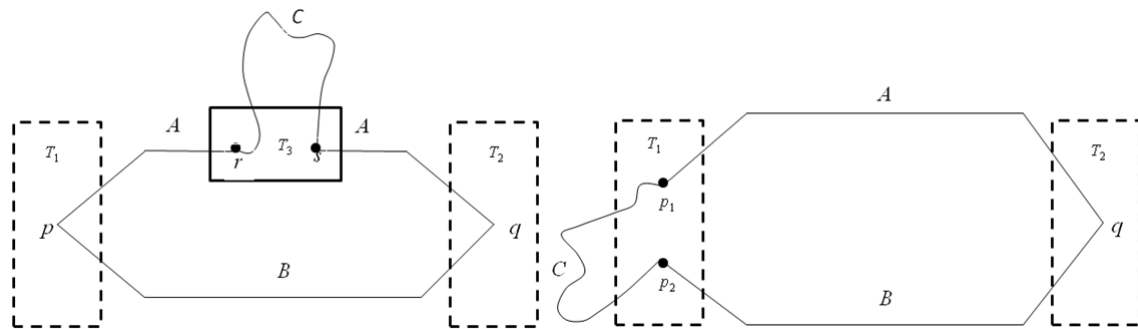


Fig. 7.1.7: Illustration of thermocouple law of intermediate metal.

**Law of intermediate metals:** Insertion of an intermediate metal into a thermocouple circuit does not affect the net emf, provided the two junctions introduced by a third metal are at identical temperatures. (Fig. 7.1.7)

**Law of intermediate temperatures:** If a simple thermocouple circuit develops an emf  $e_1$  when its junctions are at temperatures  $T_1$  and  $T_2$  and emf of  $e_2$  when the junctions are at temperatures  $T_2$  and  $T_3$ , then the same thermocouple will develop an emf  $(e_1 + e_2)$  when the junctions are at temperatures  $T_1$  and  $T_3$ , respectively.

Depending on the combination of materials used for the conductors, thermocouples are classified in different types. The selection of the material is based on cost, availability, convenience, melting point, chemical properties, stability, and output. They are usually selected based on the temperature range and sensitivity needed. Some of the classifications are given in Table 7.1.1.

Table 7.1.1: Classifications of thermocouples

<i>Type</i>	<i>Positive Conductor</i>	<i>Negative Conductor</i>	<i>Sensitivity</i>	<i>Operating Temperature Range</i>
K	Chromel	Alumel	41 $\mu\text{V}/^\circ\text{C}$	$-200^\circ\text{C}$ to $1350^\circ\text{C}$
E	Chromel	Constantan	68 $\mu\text{V}/^\circ\text{C}$	$-250^\circ\text{C}$ to $900^\circ\text{C}$
J	Iron	Constantan	55 $\mu\text{V}/^\circ\text{C}$	$-40^\circ\text{C}$ to $750^\circ\text{C}$
N	Chromium	Nickel	39 $\mu\text{V}/^\circ\text{C}$	up to $1200^\circ\text{C}$
B	Platinum	Platinum / 6% Rhodium	10 $\mu\text{V}/^\circ\text{C}$	up to $1800^\circ\text{C}$
R	Platinum	Platinum / 13% Rhodium	10 $\mu\text{V}/^\circ\text{C}$	up to $1600^\circ\text{C}$
S	Platinum	Platinum / 10% Rhodium	10 $\mu\text{V}/^\circ\text{C}$	up to $1600^\circ\text{C}$
T	Copper	Constantan	43 $\mu\text{V}/^\circ\text{C}$	$-200^\circ\text{C}$ to $350^\circ\text{C}$
C	Tungsten-5% rhenium	Tungsten-26% rhenium	30 $\mu\text{V}/^\circ\text{C}$	$0^\circ\text{C}$ to $2320^\circ\text{C}$
M	Nickel-18% Molybdenum	Nickel-6% Cobalt	30 $\mu\text{V}/^\circ\text{C}$	Up to $1400^\circ\text{C}$

## Module 7 : Lecture 2

### MEASUREMENTS IN FLUID MECHANICS (Incompressible Flow – Part II)

#### Measurement of Flow Rate and Velocity

A major requirement in application areas of fluid mechanics is the determination of flow rates and with respect to incompressible flows, they are called as *flow metering*. Based on the operating principle, pressure drop, capacity, versatility, accuracy, cost, size and level of sophistication the range varies widely. For example, a crude way of measuring flow rate of water through a household tap is through the collection of water in a bucket and noting the corresponding time. On the other hand, a sophisticated instrument may involve flow rate measurement through the propagation of sound in a flowing fluid or electromotive forces when the fluid passes through a magnetic fluid. Some of the commonly used devices are as follows;

- Pitot tube and Pitot-Static probe
- Obstruction Flow meters
- Variable-area flow meter
- Thermal Anemometers
- Miscellaneous flow devices
- Scattering devices

#### Pitot tube and Pitot-static probe

In an incompressible flow, the flow rate is generally proportional to the velocity and it is obtained from the measured pressures of the flowing medium. The total pressure of a flowing stream is expressed as,

$$p_t = p_s + p_d = p_s + \frac{1}{2} \rho V^2 \Rightarrow V = \sqrt{\frac{2(p_t - p_s)}{\rho}} \quad (7.2.1)$$

where,  $V$  is the average flow velocity and  $\rho$  is the fluid density. If measurement is made in such a way that the velocity of the flow is not disturbed, then the measured pressure indicates the *static pressure* ( $p_s$ ). On the other hand, if the measurement is made such that the flow velocity of the stream is brought to rest isentropically, then the pressure obtained becomes the *stagnation/total pressure* ( $p_t$ ). The difference

between these two pressures is the *dynamic pressure* ( $p_d$ ) which is the fundamental equation for velocity measurement. The point measurements of these two pressures are accomplished by the use of tubes (called as *probes*) joining the desired location in the flow (Fig. 7.2.1). *Pitot probes and Pitot-static probes* are the standard devices that are used widely for obtaining  $p_s$  and  $p_t$ .

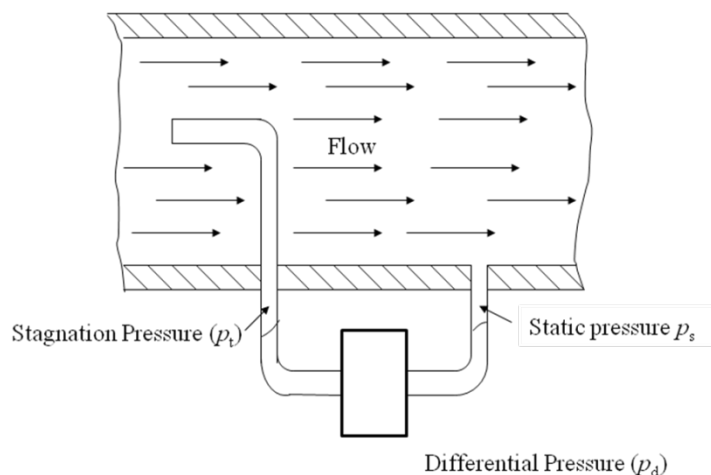


Fig. 7.2.1: Schematic representation of static and stagnation pressure measurements.

A *Pitot probe* is a simple tube with a pressure tap at the stagnation point where the flow comes to rest and thus the pressure measured at this point is the *stagnation pressure* (Fig. 7.2.2-a). The *Pitot-static probe* consists of a slender double-tube aligned with the flow and connected to a differential pressure measuring device such as manometer (Fig. 7.2.2-b). The inner tube is fully open to the flow at the nose and thus measures the stagnation pressure (point '1') while the outer tube is sealed at the nose, but has the holes on the circumference of the outer wall for measuring the static pressure (point '2'). Neglecting frictional effects in Fig. 7.2.2(c), Bernoulli's equation can be applied for the point '1 and 2' to obtain the average flow velocity as given by Eq. (7.2.1). This equation is also known as *Pitot formula*. The volume flow rate can be obtained by multiplying the cross-sectional area to this velocity.

The Pitot-static probe is a simple, inexpensive and highly reliable device because it has no moving parts. Moreover, this device can be used for velocity/flow rate measurements for liquids as well as gases. Referring to Eq. (7.2.1), the dynamic pressure (i.e. difference between stagnation and static pressure) is proportional to the density of the fluid and square of the flow velocity. When this device is used for gases, it is expected that velocity is relatively high to create a noticeable dynamic pressure because gases have low densities.

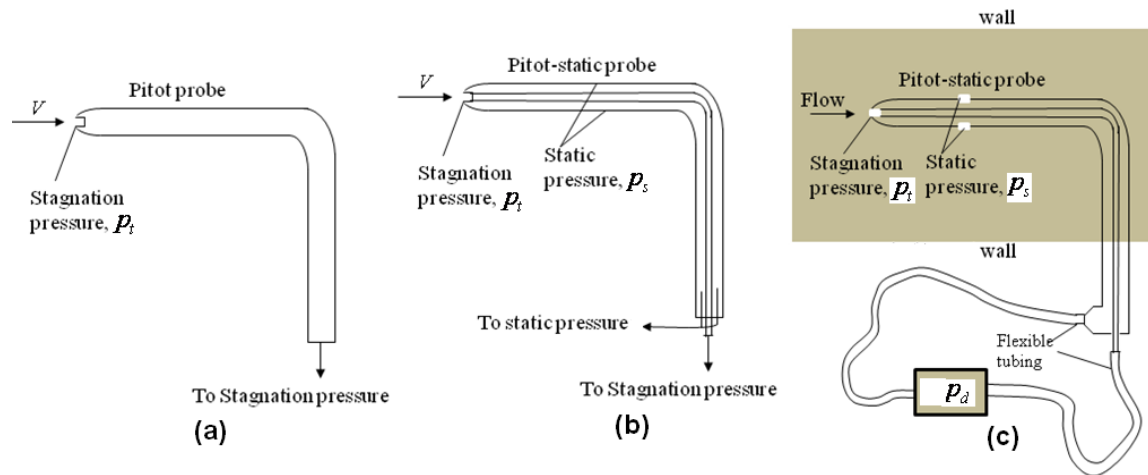


Fig. 7.2.2: (a) Pitot probe; (b) Pitot-static probe; (c) Measuring flow velocities with a Pitot-static probe.

### Obstruction Flow meters

The flow rate through a pipe can be determined by constricting the flow and measuring the decrease in pressure due to increase in velocity at the constriction. In order to illustrate this fact, consider an incompressible steady flow of fluid in a horizontal pipe area ( $A_1$ ) and diameter ( $D$ ) which is constricted to a flow area ( $A_2$ ) and diameter ( $d$ ) at certain location (Fig. 7.2.3). The mass balance and Bernoulli equation can be applied between a location before the constriction (point '1') and at the constriction site (point '2').

$$\begin{aligned} \text{Mass balance: } A_1 V_1 &= A_2 V_2 \Rightarrow V_1 = \left( \frac{A_2}{A_1} \right) V_2 = \left( \frac{d}{D} \right)^2 V_2 \\ \text{Bernoulli equation: } \frac{p_1}{\rho g} + \frac{V_1^2}{2g} &= \frac{p_2}{\rho g} + \frac{V_2^2}{2g} \quad (z_1 = z_2) \end{aligned} \quad (7.2.2)$$

Combining both the equations and solving for  $V_2$  one can obtain the expression for velocity and flow rate ( $\dot{V}$ ) at the constriction location.

$$V_2 = \sqrt{\frac{2(p_1 - p_2)}{\rho(1 - \beta^4)}}; \quad \dot{V} = A_2 V_2 = \left(\frac{\pi}{4} d^2\right) V_2 \quad (7.2.3)$$

where,  $p_1, V_1$  and  $p_2, V_2$  are the pressure and velocities at points '1 and 2', respectively and  $\beta = \frac{d}{D}$  is the diameter ratio. It is noticed from Eq. (7.2.3) that the

flow rate through a pipe can be determined by constricting the flow and measuring the decrease in pressure due to increase in velocity at the constriction site. The devices based on this principle is known as *obstruction flow meters* and widely used to measure flow rates for gases and liquids. Depending on nature of constriction, the obstruction flow meters are classified as *orifice*, *nozzles* and *venturimeter* as shown in Fig. 7.2.4.

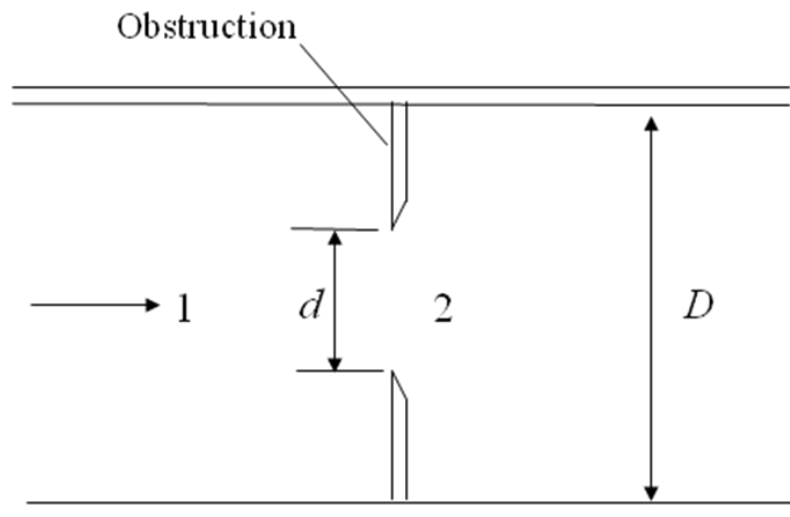


Fig. 7.2.3: Flow through a constriction in a pipe.

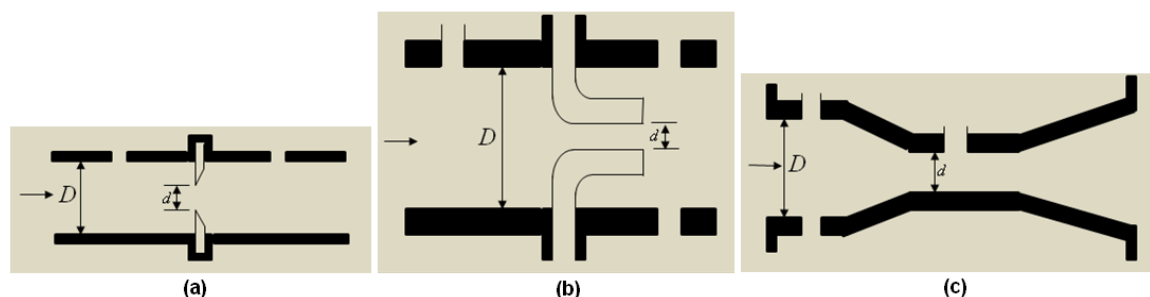


Fig. 7.2.4: Classification of obstruction flow meters: (a) orifice; (b) nozzle; (c) venturimeter.

The *orifice meter* (Fig. 7.2.4-a) has the simplest design and it occupies minimal space. It consists of a plate with a hole in the middle and this hole may be sharp-edged/beveled/rounded. The sudden change in the flow area causes a *vena-contracta* (minimum area) and thus leading to significant head loss or swirl. In the flow through *nozzles* (Fig. 7.2.4-b), the plate is replaced by a nozzle and the flow becomes streamlined. As a result, the *vena-contracta* is practically eliminated that leads to very small head losses. The most accurate measurement device in the flow meter category is the *venturi-meter* (Fig. 7.2.4-c). Its gradual contraction and expansion prevents flow separation and swirling which minimizes the head losses. However, it suffers irreversible losses due to the friction at the wall which is only about 10%.

The velocity expression in the Eq. (7.2.3) is obtained by assuming no loss and thus it is the maximum velocity that occurs at the constriction site. In reality, the velocity will be less than this value because of inevitable frictional losses. Also, the fluid stream will continue to contract past the obstruction and the *vena-contracta* is less than the flow area of the obstruction. By incorporating these two factors, a correction factor is introduced in the obstruction flow meters, which is measured experimentally. The volume flow rate is then expressed by a parameter called as *discharge coefficient* ( $C_d$ ).

$$\dot{V} = A_0 C_d V_2 = A_0 C_d \sqrt{\frac{2(p_1 - p_2)}{\rho(1 - \beta^4)}} \quad \left( A_0 = \frac{\pi}{4} d^2 \right) \quad (7.2.4)$$

The value of  $C_d$  depends on the geometrical parameter  $\beta$  and flow Reynolds number  $\left( \text{Re} = \frac{\rho V_1 D}{\mu} \right)$ . In the range of  $0.25 < \beta < 0.75$  and  $10^4 < \text{Re} < 10^7$ , the value  $C_d$  of can be approximated by the following relations;

$$\begin{aligned} \text{Orifice: } C_d &= 0.5959 + 0.0312 \beta^{2.1} - 0.184 \beta^8 + \frac{91.71 \beta^{2.5}}{\text{Re}^{0.5}} \\ \text{Nozzles: } C_d &= 0.9975 - \frac{6.53 \beta^{0.5}}{\text{Re}^{0.5}} \end{aligned} \quad (7.2.5)$$

For high Reynolds number flows ( $\text{Re} > 30000$ ), the value of  $C_d$  can be taken as 0.61 for orifice and 0.96 for nozzles. In the case of venturimeter, the of  $C_d$  ranges from 0.95 to 0.99 irrespective of flow Reynolds number and area ratio because this device in intended for streamlined design.



Relative merits of venturi meter, nozzle and orifice

- High accuracy, good pressure recovery and resistance to abrasion are the primary advantages of the venturi. The space requirement and cost of the venturi meter is comparatively higher than that of orifice and flow nozzle.
- The orifice is inexpensive and may often be installed between existing pipe flanges. However, its pressure recovery is poor and it is especially susceptible to inaccuracies resulting from wear and abrasion. It may also be damaged by pressure transients because of its lower physical strength.
- The nozzle possesses the advantages of the venturi, except that it has lower pressure recovery and it has the added advantage of shorter physical strength. It is inexpensive compared with the venturimeter but relatively difficult to install properly.

## Module 7 : Lecture 3

### MEASUREMENTS IN FLUID MECHANICS (Incompressible Flow – Part III)

#### Variable-Area Flow Meter

In the obstruction flow meters, the flow is allowed to pass through a reduced cross-sectional area ( $A_0$ ) and the corresponding pressure difference ( $p_1 - p_2$ ) is measured by using any differential pressure measuring device. The expression for volume flow rate ( $\dot{V}$ ) is given by,

$$\dot{V} = A_0 C_d \sqrt{\frac{2(p_1 - p_2)}{\rho(1 - \beta^4)}} \quad \left( A_0 = \frac{\pi}{4} d^2; \beta = \frac{d}{D} \right) \quad (7.3.1)$$

where,  $d$  and  $D$  are the smaller and larger diameters for the flow, respectively,  $C_d$  is the discharge coefficient and  $\rho$  is the density of the fluid. It may be noted from Eq. (7.3.1) that the pressure drop varies as square of the flow rate. In other words, if these devices are to be used for wide range of flow rate measurements, then the pressure measuring equipment should have capability of handling larger pressure range. By incorporating larger pressure ranges, the accuracy of the device will be poor for low flow rates i.e. the small pressure readings in that range will be limited by the pressure transducer resolution. This is the major drawback of the obstruction flow devices.

One of the solutions is to use two pressure measuring systems, one for low flow rates and the other for high flow rates. A simple, reliable and inexpensive device used for measuring flow rates for wide ranges of liquids and gases. This device is easy to install with no electrical connections and gives a direct reading of flow rate. It is known as *variable area flow meter* and also called as *rotameter/floatmeter*. It consists of a vertical tapered conical transparent tube made of glass/plastic with a *float/bob* inside the tube as shown in Fig. 7.3.1. The *bob* is free to move inside the tube and is heavier than the fluid it displaces. At any point of time, the float experiences three fundamental forces; drag, buoyancy and its own weight. With increase in flow velocity, the drag force increases and the flow velocity reduces with increase in cross-sectional area in the tapered tube. At certain velocity, the float settles at a location where enough drag ( $F_d$ ) is generated to balance the weight of the *bob* ( $W_b$ ) and

buoyancy force ( $F_b$ ). In other words, the net force acting on the *bob* is zero and thus it is in equilibrium for a given flow rate. The degree of tapering of the tube can be made such that the vertical rise changes linearly with the flow rate and a suitable scale outside the tube is fixed so that the flow rate can be determined by matching the position of float.

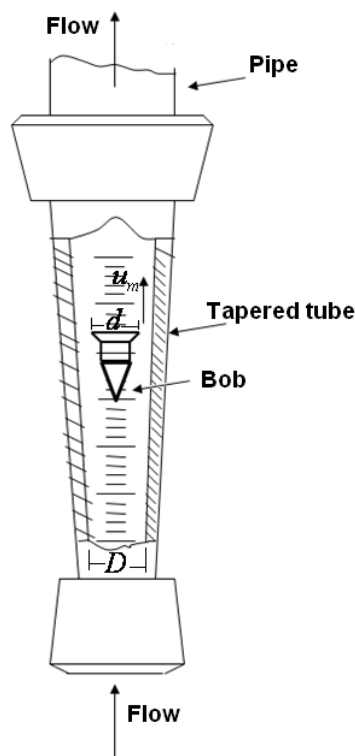


Fig. 7.3.1: Schematic diagram of a rotameter.

At equilibrium state, the force balance on bob can be written by the following expression;

$$F_d + F_b = W_b \quad (7.3.2)$$

By definition, all these forces terms can be expressed in the following form;

$$F_d = C_D A_b \frac{\rho_f u_m^2}{2}; F_b = \rho_f V_b g; W_b = \rho_b V_b g \quad (7.3.3)$$

where,  $V_b$  is the total volume of the bob,  $A_b$  is the frontal area of the bob,  $u_m$  is the mean flow velocity in the annular space between the bob and tube,  $C_D$  is the drag coefficient,  $g$  is the acceleration due to gravity,  $\rho_f$  and  $\rho_b$  are the fluid density and

float density, respectively. Both Eqs (7.3.2 & 7.3.3) can be combined to obtain the expression for  $u_m$  and subsequently volume flow rate ( $\dot{V}$ ).

$$u_m = \left[ \frac{1}{C_D} \frac{2gV_b}{A_b} \left( \frac{\rho_b}{\rho_f} - 1 \right) \right]^{\frac{1}{2}} \quad (7.3.4)$$

and  $\dot{V} = Au_m$ ;  $A = \frac{\pi}{4} \left[ (D + ay)^2 - d^2 \right]$

Here,  $A$  is the annular area,  $D_f$  is the diameter of the tube at inlet,  $d$  is the maximum bob diameter,  $y$  is the vertical distance from the entrance and  $a$  is the constant indicating the tube taper. Since the drag coefficient depends on the Reynolds number and fluid viscosity, special bob may be used to have constant drag coefficient. It is also possible to decide appropriate geometrical dimensions so that a linear relation is obtained for the expression given by the Eq. (7.3.4).

$$\dot{m} = C_1 y \sqrt{(\rho_b - \rho_f) \rho_f}; \quad C_1 \text{ is a constant for rotameter.} \quad (7.3.5)$$

Since the response of rotameter is linear, its resolution is same for both higher and lower flow rates. The accuracy for these types of devices is typically  $\pm 5\%$ . However, rotameters have certain drawbacks such as vertical installation and inability for measurements of opaque fluids because the float may not be visible.

### Thermal Anemometers

The *thermal anemometers* are often used in research applications to study rapidly varying flow conditions. When, a heated object is placed in a flowing fluid, it tends to lose heat to the fluid. The rate, at which the heat is lost, is proportional to the flow velocity. If the object is heated to a known power and placed in the flowing fluid, then heat will be lost to the fluid. Eventually, the object will reach to a temperature which is decided by the rate of cooling. However, if the temperature of the object is to be maintained constant, then the input power needs to be changed which is proportional to the fluid velocity. So, the heating power becomes a measure of velocity. The concept of using thermal effects to measure the flow velocity was introduced in late 1950s. The *thermal anemometers* have extremely small sensors and are useful to

measure instantaneous velocity at any point in the flow without disturbing the flow appreciably (Fig. 7.3.2).

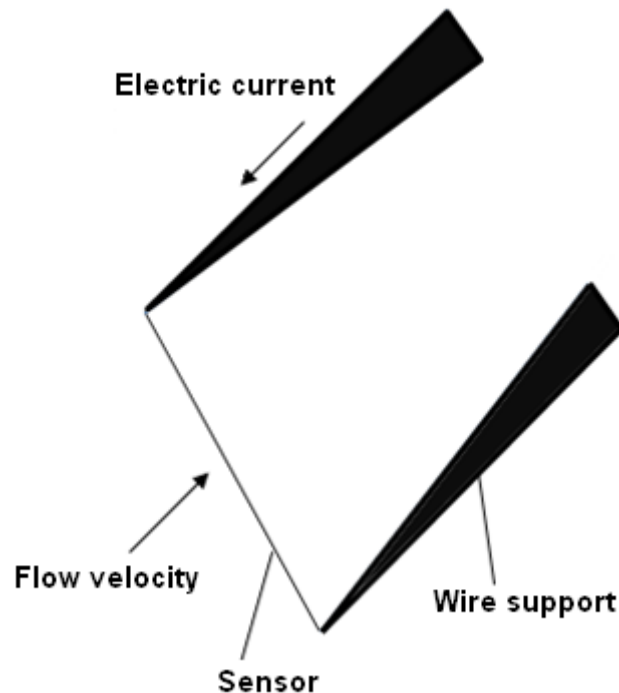


Fig. 7.3.2: Operating principle of a thermal anemometer.

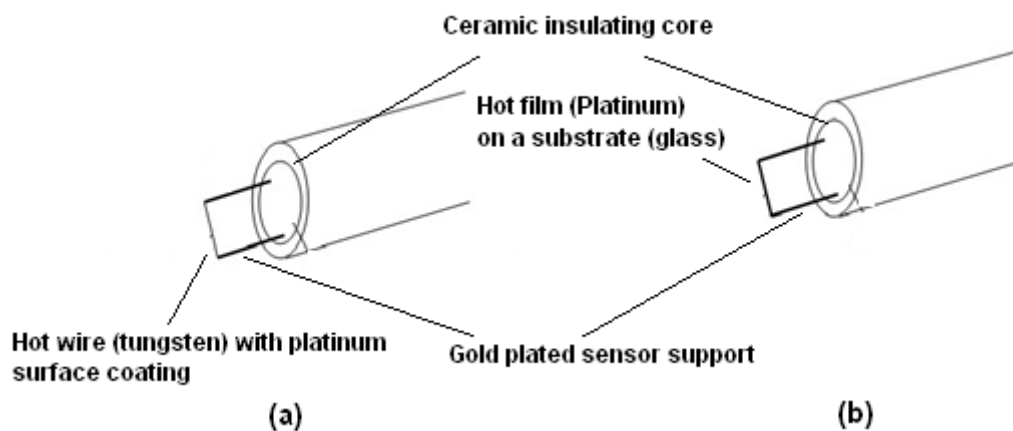


Fig. 7.3.3: A hot-wire/hot film thermal anemometer with its support system:

(a) hotwire; (b) hot-film.

The schematic diagram of a hot-wire/hot-film probe is shown in Fig. 7.3.3. A thermal anemometer is called a *hot-wire anemometer* when the sensing element is a wire. It is called as a *hot-film anemometer* if the sensor is a thin metallic film. For a hot-wire anemometer, the sensing element has a diameter of few micron and length of 2mm. In the case of *hot-film anemometer*, the sensing element is of  $0.1\mu\text{m}$  thick and mounted on a ceramic support. The sensing element is usually made out of platinum, tungsten or platinum-iridium alloy.

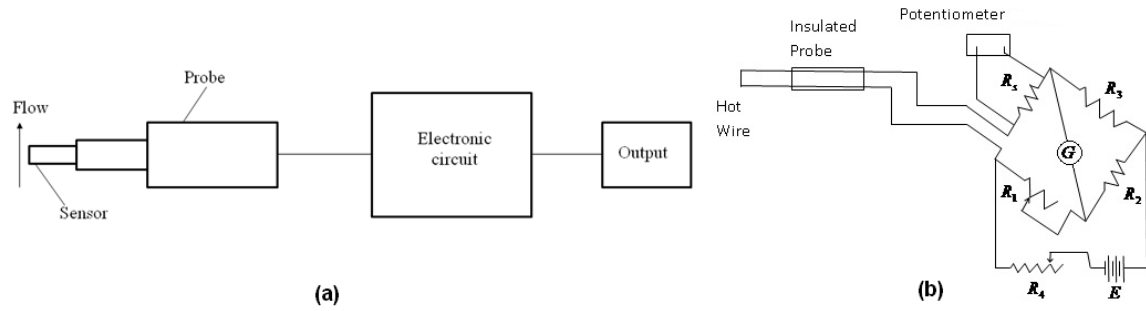


Fig. 7.3.4: (a) Schematic representation of anemometer measurement; (b) Anemometer feedback controlled circuit.

Both hot-wire and hot-film probes are operated using a feed-back controlled bridge (Fig. 7.3.4) that controls the input power to the probe to maintain constant temperature when there is a change in fluid velocity. The higher is the flow velocity, the more will be heat transfer from the sensor and more voltage/power will be required for the sensor. When the sensor is maintained at constant temperature, the thermal energy remains constant. So, the electrical heating ( $\dot{q}_E$ ) of the sensor is equal to the rate of heat loss through convection ( $\dot{q}_C$ ) and is often governed by *King's law*.

$$\begin{aligned}\dot{q}_C &= (a + bV^{0.5})(T_w - T_\infty) \\ \dot{q}_E &= i^2 R_{ref} \left[ 1 + \alpha (T_w - T_{ref}) \right]\end{aligned}\quad (7.3.6)$$

where,  $i$  is the electric current in the circuit,  $V$  is the flow velocity,  $\alpha$  is the temperature coefficient of resistance,  $a$  and  $b$  are the calibration constants,  $T_w$ ,  $T_\infty$  and  $T_{ref}$  are the wire temperature, free stream fluid temperature and reference temperature, respectively. With appropriate calibration, Eq. (7.3.6) can be expressed through a close correlation between flow velocity ( $V$ ) and voltage ( $E$ ).

$$E^2 = A + BV^n; \quad A, B \text{ and } n \text{ are calibration constants.} \quad (7.3.7)$$

One of the important applications includes the turbulence measurements where the velocity fluctuations are important. Two or more wires at one point in the flow can make simultaneous measurements of the fluctuating components. The thermal anemometers have distinct advantages of measuring very high velocities ( $\sim 1000\text{m/s}$ ) with excellent spatial and temperature resolution for liquids as well as gases. The hot film probes are extremely sensitive to fluctuations in the fluid velocity and have been used for measurements involving frequencies as high as 50 kHz. The *time constants* of the order of 1ms can be obtained with hot-wire probes operating in air. Moreover, simultaneous measurement of velocity components (three-dimensional) can be done by aligning three sensors on a single probe.

## Module 7 : Lecture 4

### MEASUREMENTS IN FLUID MECHANICS (Incompressible Flow – Part IV)

#### Miscellaneous Measuring Devices

The preceding section covers the common types of flow meters such as obstruction devices and rotameter. There are few additional devices that are used for specific applications and these devices can be made such that outputs that vary linearly with flow rate. Some of the special classes of these devices are briefly discussed here.

#### Electromagnetic flow meters

When a conductor is moved in a magnetic field, an electromotive force is developed due to magnetic induction. The voltage induced across the conductor (EMF) while moving right angles to the magnetic field is proportional to the velocity of the conductor. This principle is known as Faraday's law and stated by the following equation;

$$EMF = BLV \times 10^{-8} \quad (7.4.1)$$

where,  $B$  is the magnetic flux density (gauss),  $L$  is the length of the conductor (cm) and  $V$  is the velocity of the conductor (cm/s). If the conductor is replaced by a conducting fluid, then  $V$  may be replaced by flow velocity.

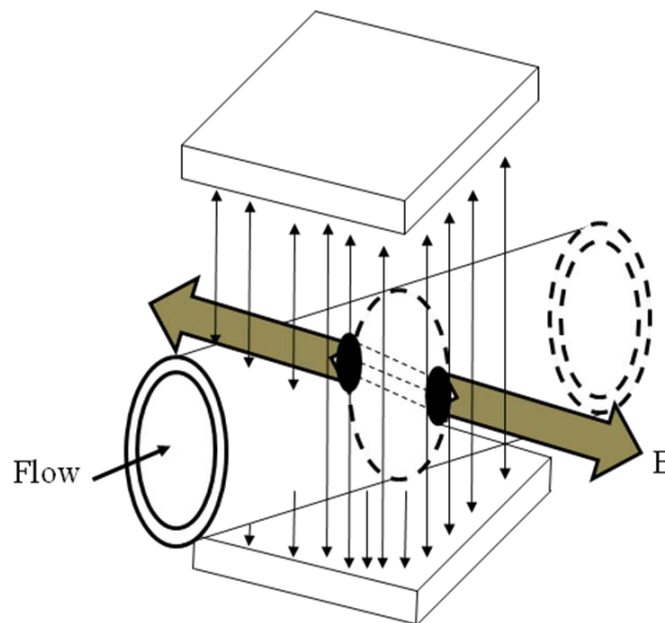


Fig. 7.4.1: Operating principle of an electromagnetic flow meter.



A *full flow electromagnetic flow meter* is a non-intrusive device consisting of a magnetic coil that encircles the pipe containing a flowing fluid (conductive), as shown in Fig. 7.4.1. Two electrodes are drilled and flush-mounted into the inner surface of the pipe but do not interfere with the flow. These electrodes are then connected to the voltmeter that measures the electric potential difference due to the flow velocity of the conducting fluid.

Electromagnetic flow meters are best-suited for measuring flow velocities of liquid metal such as mercury, sodium, and potassium and find applications in nuclear reactors. They can also be used for liquids of poor conductors if they contain adequate amount of charged particles. Flow rate measurement of corrosive liquids, slurries and fertilizers are also possible by electromagnetic flow meters. Commercial magnetic flow meters have rated accuracies of 0.5% to 1%.

### **Turbine meters**

It is a rotating-wheel type magnetic flow meter which is used to measure water flows in rivers and streams. As the fluid moves through the meter, it causes a rotation of the small turbine wheel. A permanent magnet is encased in the rotor body such that the change in permeability is noticed when the rotor blade passes through the pole of the coil. The change in the permeability of the magnetic circuit produces a voltage pulse at the output measuring terminal. The rotor motion is proportional to the volume flow rate and is captured by an inductive coil. A flow coefficient ( $K$ ) for the turbine meter may be defined based on the flow rate ( $\dot{V}$ ) and kinematic viscosity of the fluid.

$$\dot{V} = \frac{f}{K}; \quad f \text{ is the pulse frequency.} \quad (7.4.2)$$

This particular device indicates the flow accurately within  $\pm 0.5\%$  over wide range of flow rates.

### Vortex flow meters

When a flow stream encounters an obstruction in its path, the fluid separates and swirls around the obstruction. This leads to formation of vortex and it is felt for some distance downstream. It is a very familiar situation for turbulent flows and a short cylinder placed in the flow sheds the vortices along the axis. If the vortices are periodic in nature, then the shedding frequency is proportional to the average flow velocity. In other words, the flow rate can be determined by generating vortices in the flow by placing an obstruction along the flow and measuring the shedding frequency. For an incompressible fluid, a dimensionless parameter known as *Strouhal number* ( $St$ ) is defined as function of vortex shedding frequency ( $f_s$ ), characteristic dimension of the obstruction ( $l$ ) and the velocity of flow ( $V$ ) impinging the obstruction.

$$St = \frac{f_s l}{V} \quad (7.4.3)$$

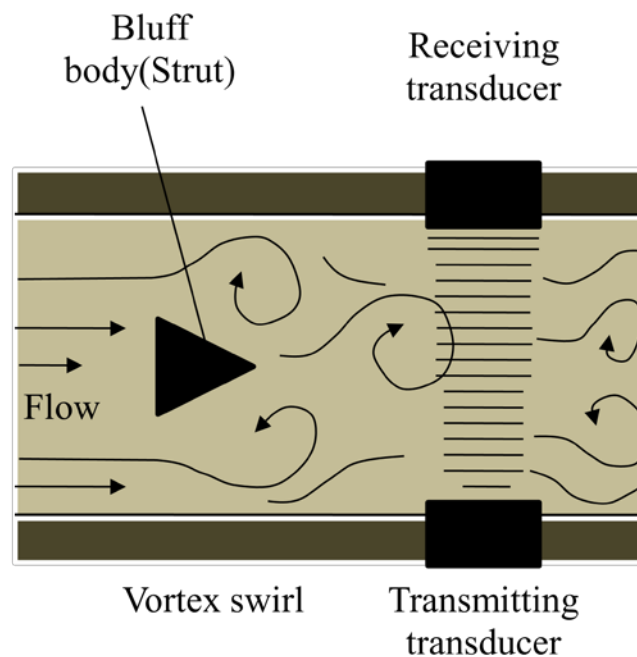


Fig. 7.4.2: Operation of a vortex flow meter.

A vortex flow meter works on the above principle is shown in Fig. 7.4.2. It consists of a bluff body placed in the flow that serves as vortex generator and a detector placed at certain distance downstream on the inner surface of casing records the shedding frequency. A piezoelectric sensor mounted inside the vortex shedder detects the vortices and subsequently amplified to indicate either instantaneous flow

rate or total flow over selected time interval. With prior knowledge of calibration constant ( $St$ ) and characteristic length dimension of the bluff body, the average flow velocity can be obtained. The vortex flow meters operate reliably between the Reynolds numbers of  $10^4$  to  $10^7$  with an accuracy of 1%. It is generally not suitable for use of high viscous liquids.

### Ultrasonic flow meters

When a disturbance is created in the flowing fluid, it generates sound waves that propagate everywhere in the flow field. These waves travel faster in the flow direction (downstream) compared to the waves in the upstream direction. As a result, the waves spread out downstream while they are tightly packed upstream. The difference between the number of waves in upstream and downstream is proportional to the flow velocity. The ultrasonic flow meters operate on this principle using sound waves in the ultrasonic range ( $\sim 1\text{MHz}$ ). Its operation mainly depends on the ultrasound waves being reflected and discontinuities in the density. Also, solids, bubbles and any discontinuity in the liquid will reflect the signal back to the receiving element. So, the device requires that the liquid contains at least 25ppm (parts per million) of particles or bubbles having diameters of  $30\mu\text{m}$  or more. There are few distinct advantages of ultrasonic flow meters such as easy installation, non-intrusive type measurement and negligible pressure drop since it does not interfere the flow. Two basic kinds of ultrasonic flow meters include *transit time* and *frequency shift* flow meters.

The *transit time flow meter* (Fig. 7.4.3-a) involves two transducers located at certain distance ( $l$ ) that alternatively transmits and receive ultrasonic sound waves, in the direction of the flow as well as in the opposite direction. The travel time for each direction can be measured accurately and the difference ( $\Delta t$ ) can be estimated. The average flow velocity ( $V$ ) can be determined from the following relation;

$$V = K l (\Delta t); K \text{ is a constant} \quad (7.4.4)$$

The *frequency shift* flow meter (Fig. 7.4.3-b) is normally known as *Doppler-effect* ultrasonic flow meter that measures average velocity along the sonic path. The piezo-electric transducers placed outside the surface of the flow transmits sound waves through the flowing fluid that reflects from the inner wall of the surface. By capturing the reflected signals, the change in frequency is measured which is proportional to the flow velocity.

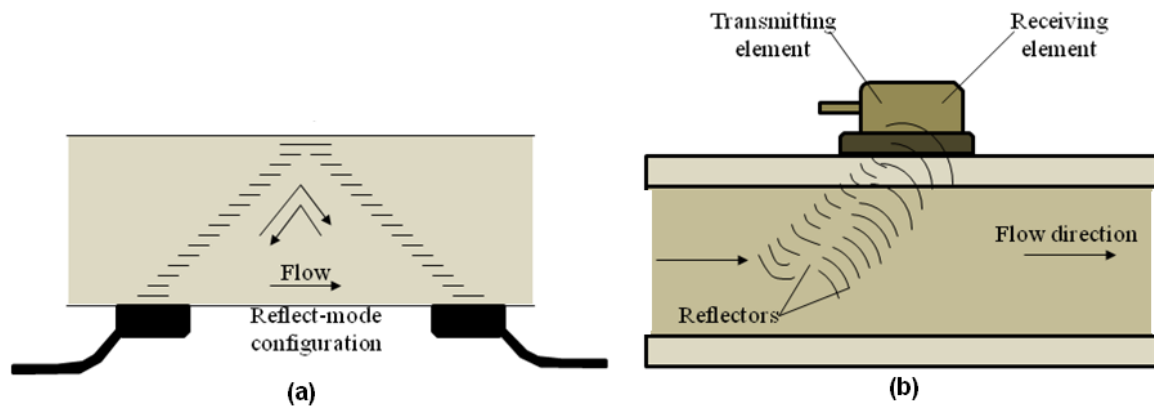


Fig. 7.4.3: Basic principle of an ultrasonic flow meter: (a) Transit time flow meter; (b) Frequency shift flow meter.

### Laminar flow meter

It is constructed through the collection of small tubes (diameter  $d$  and length  $l$ ) of sufficiently small sizes (Fig. 7.4.4) so that laminar flow is ensured and the entrance/exit losses occur within the tube assembly. Thus, the flow rate for a given fluid (viscosity  $\mu$ ) becomes direct function of pressure difference ( $p_2 - p_1$ ).

$$\dot{V} = \frac{\pi d^4 (p_1 - p_2)}{128 \mu L} = \frac{\pi d^4 \Delta p}{128 \mu L} \quad (7.4.5)$$

Since the flow is laminar, the Reynolds number ( $Re_d$ ) is within 2000. One may rewrite the expression of Reynolds number as follows;

$$Re = \frac{\rho u_m d}{\mu} = \frac{\rho \dot{V}}{(\pi/4) d^2} \left( \frac{d}{\mu} \right) = \frac{4 \dot{V} \rho}{\pi d \mu} \quad (7.4.6)$$

Combining the Eqs (7.4.5 & 7.4.6), the design selection of  $l$  and  $d$ , for a laminar flow meter can be set for certain range of pressure drop and flow Reynolds number.

$$\Delta p = p_1 - p_2 = \frac{128 (Re) \mu^2 L}{4 \rho d^3} \quad (7.4.7)$$

In contrast to obstruction flow devices, the volume flow has a linear relation with pressure drop for a *laminar flow meter*. It allows the operation of this device for wide range of flow rates for a given pressure differential, within an uncertainties of  $\pm 4\%$ . However, being small in sizes, the laminar tube elements are subjected to clogging when used with dirty fluids.

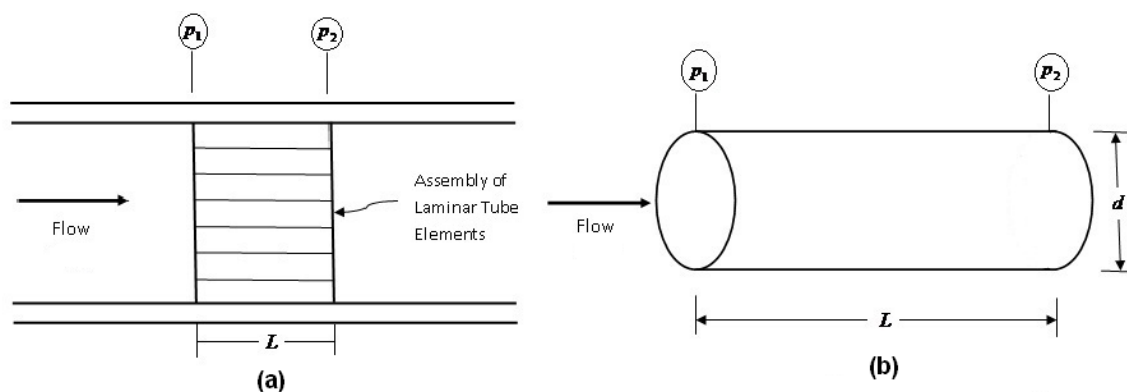


Fig. 7.4.4: (a) Basic principle of a laminar flow meter; (b) A laminar flow element.

### Thermal mass flow meter

A direct measurement of mass flow of gases can be accomplished through thermal energy transfer (Fig. 7.4.5). The flow takes place through a precision tube fitted with an electric heater. Both upstream and downstream sections have externally wound resistance temperature detectors (RTDs) typically made out of platinum with probe diameter of about 6mm. The first sensor measures the temperature of the gas flow at the point of immersion while the second sensor is heated to a temperature of  $20^\circ\text{C}$  above the first sensor. As a result, the heat transfer to the gas from the second sensor takes place through convection which is proportional to the *mass velocity* ( $\rho u$ ) of the gas. The two sensors are connected to a Wheatstone bridge circuit for which the output voltage is proportional to the *mass velocity*. This circuit can be specially designed so that linearly varying output can be obtained from the circuit. The experiment is normally performed with nitrogen and a calibration factor is obtained for subsequent use of other gases.

It is to be noted that the *mass velocity* of the gas is measured at the point of immersion. For the flow system with varying velocities, several measurements are necessary to obtain an integrated mass flow across the channel. Velocities of the gases in the range of 0.025m/s to 30m/s can be measured with this device within an uncertainty level of  $\pm 2\%$ .

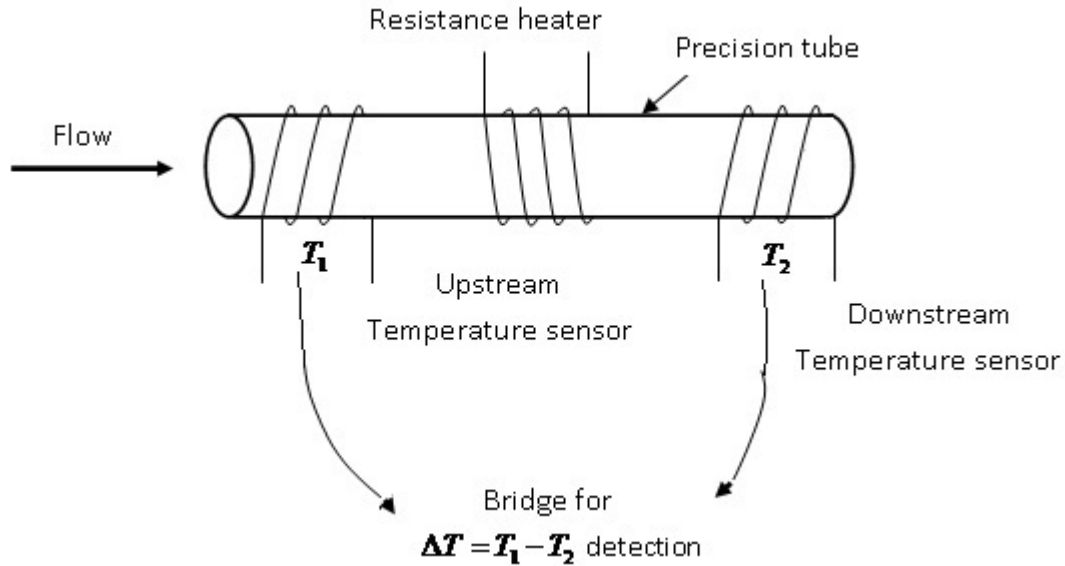


Fig. 7.4.5: Basic principle of a thermal mass flow meter.

### Scattering Devices

All the measurement techniques discussed earlier, determine the velocity by disturbing the flow. In some cases, the disturbance is very less (such as ultrasonic flow meter and thermal anemometers) while in other cases (orifice, pitot probe etc.), sufficient care to insert the measuring device to minimize the disturbances. So they are classified as *intrusive based* measurements. The modern instrumentation method used optical technique to measure the flow velocity at any desired location without disturbing the flow. So they are called as *non-intrusive based* measurement and works on the principle of scattering light and sound waves in a moving fluid. By measuring the frequency difference between scattered and un-scattered wave, particle/flow speed can be found. The *Doppler frequency shift* ( $\Delta f$ ) is responsible for this change in the speed and is illustrated in Fig. 7.4.6.

$$\Delta f = \left( \frac{2V}{\lambda} \right) \cos \beta \sin \left( \frac{\alpha}{2} \right) \quad (7.4.8)$$

where,  $V$  is the particle velocity,  $\lambda$  is the wavelength of original wave before scattering,  $\alpha$  and  $\beta$  are the angles shown in Fig. 7.4.6. The important aspect of the Eq. (7.4.8) is the proportionality between  $\Delta f$  and  $V$ . If  $\Delta f$  can be measured, then one can obtain the particle speed. Since, the particle moves with the flow, so the particle speed is equal to flow speed. Since, the laser light and ultrasonic waves have relatively high frequencies, they are normally used for measuring flow velocity because the Doppler shift will be only a small fraction compared to original frequency. *Laser Doppler Velocimetry (LDV)* and *Particle Image Velocimetry (PIV)* are the optical techniques that work on the principle of *Doppler shift*.

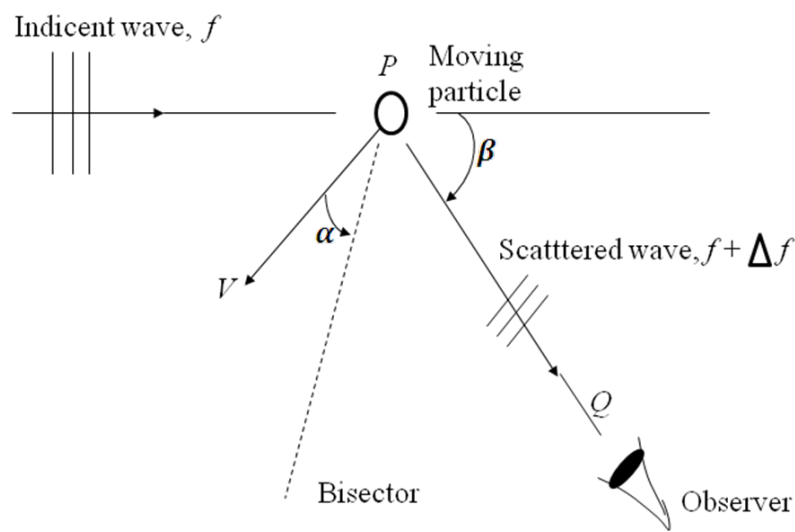


Fig. 7.4.6: Illustration of Doppler shift for a moving fluid particle.

**Laser Doppler Velocimetry:** It is also termed as Laser Velocimetry (LV) or Laser Doppler Anemometry (LDA). The operating principle of LDV is based on sending a highly coherent monochromatic light beam towards a fluid particle. The monochromatic light beam has same wavelengths and all the waves are in phase. The light reflected from the fluid particle wave will have different frequencies and the change in frequency of reflected radiation due to *Doppler effect* is the measure of fluid velocity. A basic configuration of a LDV setup is shown in Fig. 7.4.7. The laser power source is normally a helium-neon/argon-ion laser with a power output of 10mW to 20W. The laser beam is first split into two parallel beams of equal intensity by a mirror and beam-splitters. Both the beams pass through a converging lens that focuses the beams at a point in the flow. The small fluid volume where the two beams intersect is the measurement volume where the velocity is measured. Typically, it has a dimension of 0.1mm diameter and 0.5mm long. Finally, the frequency information

of scattered and unscattered laser light collected through receiving lens and photo-detector, is converted to voltage signal. Subsequently, flow velocity ( $V$ ) is calculated.

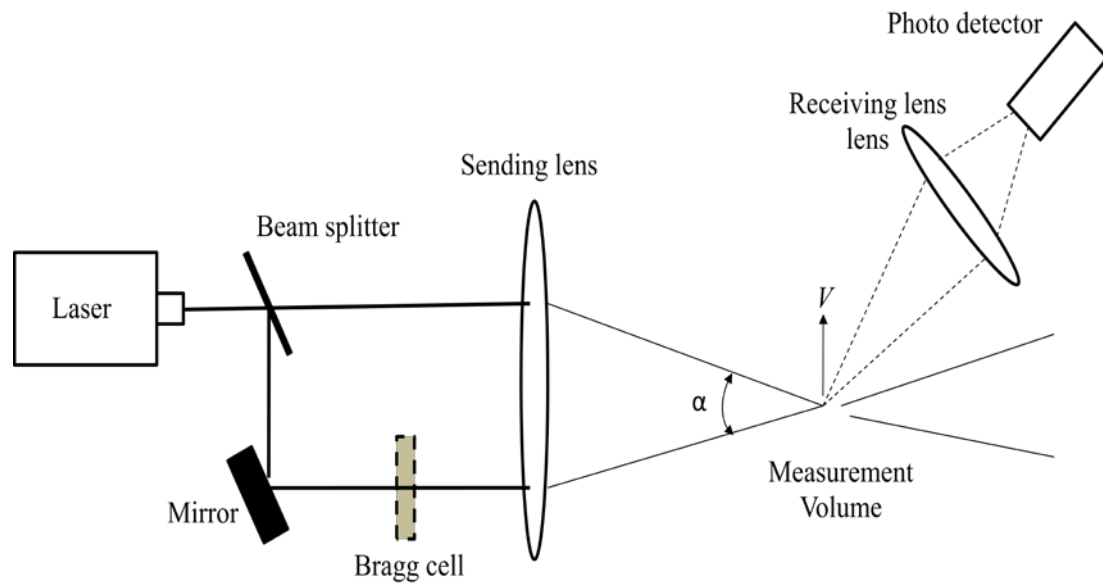


Fig. 7.4.7: Schematic representation of a LDV setup.

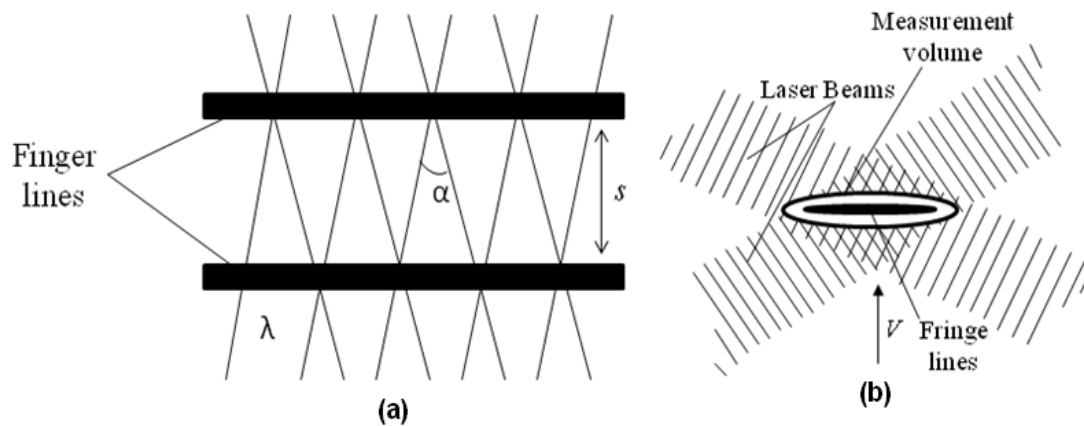


Fig. 7.4.8: Interference of laser beams: (a) Formation of fringes; (b) Fringe lines and wavelengths.

When the waves of two beams interfere in the measurement volume, it creates bright fringes when they are in phase and dark fringes when they are out of phase. The bright and dark fringes form lines parallel to the mid-plane between two incident laser beams as shown in Fig. 7.4.8(a). The spacing between fringe lines ( $s$ ) can be viewed as wavelength of fringes ( $\lambda$ ) as shown in Fig. 7.4.8(b).

$$\Delta f = \frac{V}{s} = \frac{2V \sin(\alpha/2)}{\lambda} \quad (7.4.9)$$

It is the fundamental LDV equation that shows the flow velocity proportional to the frequency.



Particle Image Velocimetry (PIV): It is a double-pulsed laser technique used to measure instantaneous velocity distribution in a plane of flow by determining the displacement of particles in that plane during a short time interval. The all other techniques such as LDV and thermal anemometry, measure the velocity at a point while PIV provides the velocity values simultaneously throughout entire cross-section through instantaneous flow field mapping.

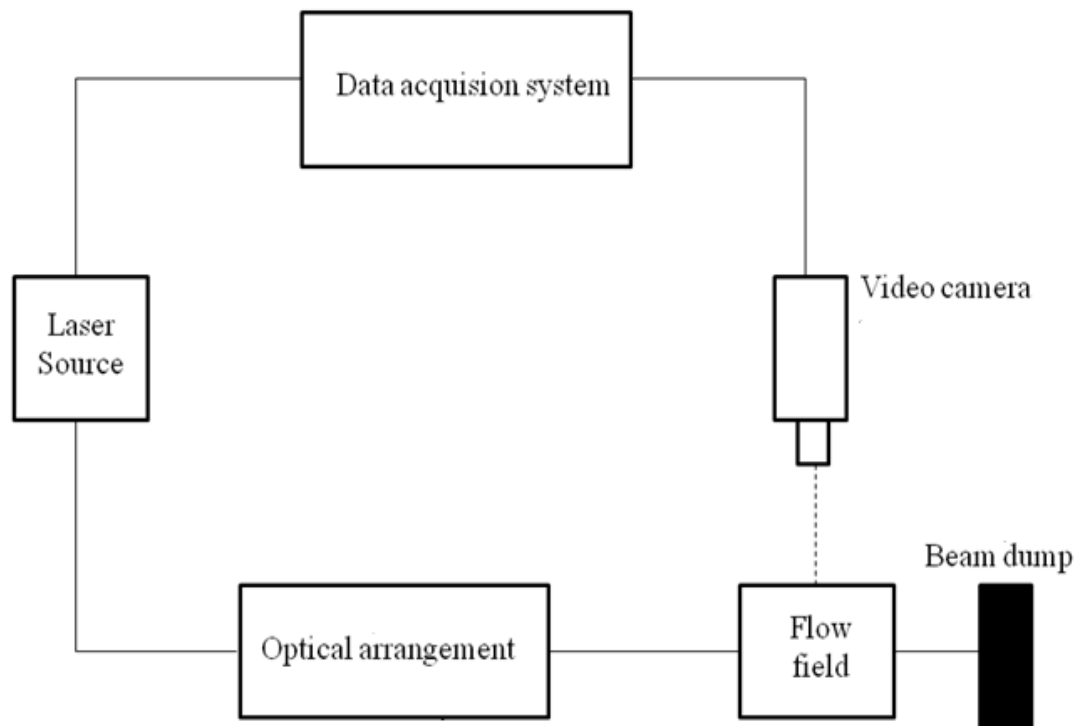


**Fig. 7.4.9: Experimental arrangement of a PIV system.**

The PIV technique for velocity measurement is based on flow visualization and image processing as shown in Fig. 7.4.9. The first step is to trace the flow with suitable seed particles in order to obtain the pathlines of fluid motion. A pulse of laser light illuminates certain region of flow field at any desired plane and the photographic view is recorded digitally by using a video camera positioned at right angle to the plane. After a short interval of time ( $\Delta t$ ), the particles are illuminated again through the laser light and the new positions are recorded. Using the information of both the images, the particle displacement ( $\Delta s$ ) is determined and subsequently the magnitude of velocity ( $\Delta s / \Delta t$ ) of the particle in the plane is calculated.

A variety of laser sources such as argon, copper vapour and Nd-YAG can be used with PIV system, depending on the requirements for pulse duration, power and time between the pulses. Silicon carbide, titanium dioxide and polystyrene latex particles are few categories of seed particles that are used depending on the type of fluid (liquid/gas). In addition to velocity measurement, the PIV is capable of measuring other flow properties such as vorticity and strain rates. The measurements can be extended to supersonic flows, explosions, flame propagation and unsteady flows. The accuracy, flexibility and versatility are the few distinct advantages of a PIV system.

## **Module 7 : Lecture 5**

### **MEASUREMENTS IN FLUID MECHANICS**

#### **(Compressible Flow – Part I)**

#### **Introduction**

The compressible flows are normally characterized as variable density flows. Pressure gradient, variable area, heat exchange and friction are few mechanisms that can change the density during a flow. But the conditions will vary for liquids and gases. For instance, the pressure gradient causes predominant change in the velocity keeping density as constant for liquids. In the other hand, the change in pressure can cause substantial velocity and density change for gases. When the density variation is less than 5%, the gases are still in the incompressible limit and the measurement techniques discussed earlier can be extended to the gases as well. However, if the density variation is substantial (more than 5%), then the measurement methods are different. The incompressible limit fails when the Mach number ( $M$ ) of the flow is more than 0.3 and the flow remains subsonic till  $M = 1$ . If the Mach number of the flow is progressively increased, then one may reach the supersonic ( $M > 1$ ) and hypersonic ( $M > 5$ ) limits. In other words, the variation in density is normally associated with high speed flows.

In the compressible flow measurements category, some of the flow parameters such as pressure, temperature are measured directly while others are calculated from the measured parameters using gas dynamic relations. When the measurements are performed for supersonic/hypersonic flows, a shock wave remains attached to the body geometry across which the static pressure, temperature and density variations are very high. Hence, the measured parameters only provide the information that prevail after the shock. Using shock wave relations, indirect calculation can be made to infer the desired flow parameters. Moreover, many advance measurement techniques involve flow field visualization through density variation to get back the information of pressure and velocity. Some of the basic compressible flow measurement techniques are discussed here.

## Measurement of Temperature

In general, the static temperature along with the pressure determines the thermodynamic state of fluid at any instant. With compressible flow field, the temperature and velocity of the flow is normally very high. In order to get the static temperature, the measuring device must travel at the fluid velocity without disturbing the flow which is quite unrealistic. So, the indirect determination of static temperature measurement is done by using thermocouples by exposing directly into the flow or mounting them on the wall surface. At any case, the flow disturbance due to obstruction of temperature sensing device should be minimized.

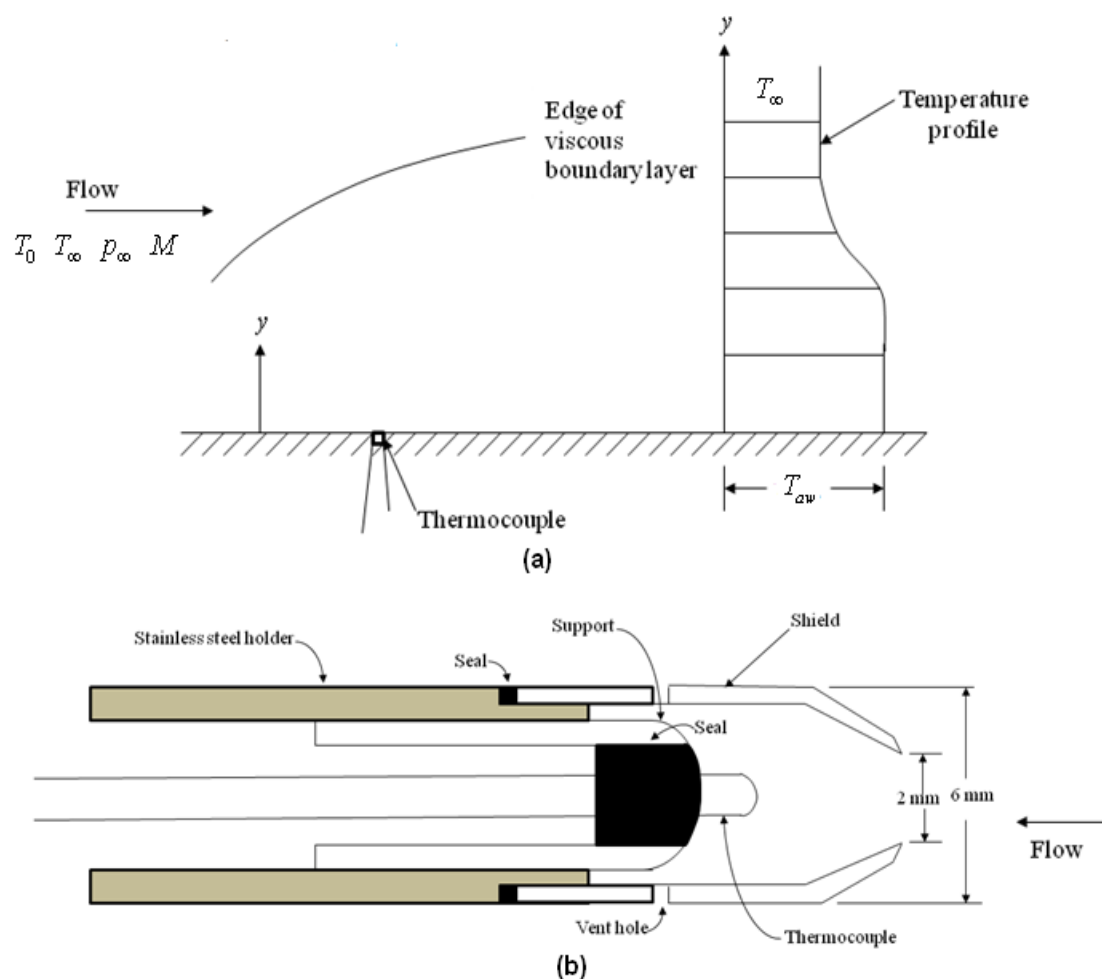


Fig. 7.5.1: Schematic diagram of temperature measurement for compressible flows: (a) thermocouple located at the wall surface; (b) temperature probe facing the flow.

The thermocouple is a simplest device for performing stagnation temperature measurements of high speed gaseous streams in a compressible flow (Fig. 7.5.1). The thermocouple located at the wall surface lies inside the viscous boundary layer at a fixed wall (Fig. 7.5.1-a). Due to viscous effects, no-slip conditions need to be satisfied at the wall and the flow velocity is zero at the wall surface. At the same time, if the

wall surface is insulated, then the temperature measured at the wall is called as *adiabatic wall temperature* ( $T_{aw}$ ). Another method is to design a probe which is inserted into the flow by minimizing the obstruction (Fig. 7.5.1-b). It consists of a diffuser which decelerates the velocity to a low value so that the fluid reaches the stagnation state at the thermocouple location. If sufficient care is made for suitable design of the probe, then it represents a thermodynamic state where the gas comes to rest isentropically (i.e. no heat exchange between the probe and surroundings). Then, the probe indicates the stagnation temperature ( $T_0$ ) given by the following isentropic expression;

$$T_0 = T_\infty + \frac{V_\infty^2}{2c_p} \quad (7.5.1)$$

where,  $c_p$  is the specific heat of the fluid at constant pressure,  $V_\infty$  and  $T_\infty$  are the velocity and static temperature of the free stream fluid, respectively.

From, aerodynamic point of view, when the gas passes over the probe, a boundary layer is likely to be formed due to velocity and temperature gradient. The velocity gradient gives rise to shear stress resulting in fluid friction and heat dissipation within the boundary layer. So, the probe will feel a temperature above the stagnation temperature. At the same time, the temperature gradient in the boundary layer gives rise to heat loss from the probe. The net effect of these two phenomena has an opposite trend to cancel each other. The non-dimensional parameter, Prandtl number  $\left( \text{Pr} = \frac{\mu c_p}{k} \right)$ , representing the ratio of shearing effects to the heat transfer effects is taken into account in the calculation of gas temperature. Since, the Prandtl number for the gases is less, the heat conduction from the probe surface dominates and the probe generally feels the temperature less than the stagnation temperature ( $T_0$ ). At the same time, if the probe is properly insulated and there is no heat exchange through conduction by stem and radiation, then the probe temperature will be the *adiabatic wall temperature* ( $T_{aw}$ ). This deviation in the probe reading and isentropic stagnation temperature is expressed by *adiabatic recovery factor* ( $R$ ).

$$R = \frac{T_{aw} - T_\infty}{T_0 - T_\infty} \Rightarrow \frac{T_{aw}}{T_\infty} = 1 + R \left( \frac{T_0}{T_\infty} - 1 \right) = 1 + R \left( \frac{\gamma - 1}{2} \right) M^2 \quad (7.5.2)$$

Here, the stagnation to static temperature ratio ( $T_0/T_\infty$ ) is obtained from isentropic relation. When the Prandtl number is unity, the adiabatic wall temperature becomes equal to stagnation temperature. The *adiabatic recovery factor* expressed in Eq. (1) applies to the case when the Prandtl number is not unity. In most cases, it is always less than 1 and is related to *adiabatic recovery factor* as given below;

$$\begin{aligned} \text{Laminar compressible boundary layer: } R &= \text{Pr}^{1/2} \quad (= 0.72 \text{ for air}) \\ \text{Turbulent compressible boundary layer: } R &= \text{Pr}^{1/3} \quad (= 0.9 \text{ for air}) \end{aligned} \quad (7.5.3)$$

With respect to measurement limitations, another deviation may arise if the probe protrudes into the flow. Here, there are possibility of heat exchange through conduction by the stem of the probe and radiation from the probe. So the temperature measured by the probe is  $T_p$  instead of  $T_0$  or  $T_{aw}$ . To account this fact, a correction factor ( $K$ ) is introduced, which is defined by the following equation.

$$K = \frac{T_p - T_\infty}{T_0 - T_\infty} \quad (7.5.4)$$

In a particular flow field, if the temperature probe is designed such that heat loss from the sensor is negligible, then the value of  $K$  is equal to  $R$  as it is the measure of transport phenomena in the boundary layer and it gets altered by the shape of the instrument. The various temperature discussed above in a compressible flow is shown in Fig. 7.5.2.

When the measurement is performed for supersonic flow stream, a detached shock is formed at a certain distance in front of the probe (Fig. 7.5.3). Since the flow across a shock is adiabatic, the stagnation temperatures remain the same before and after the shock. So, the temperature measurement remains unaffected.

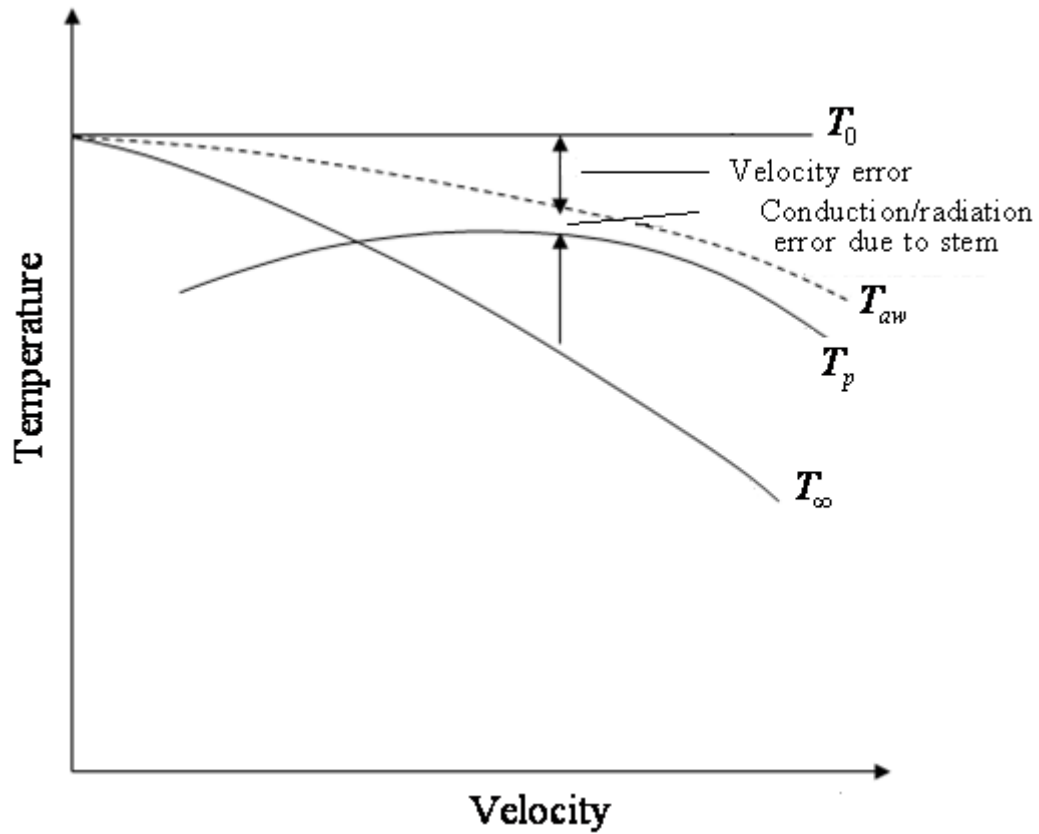


Fig. 7.5.2: Representation of temperature trends in a compressible flow.

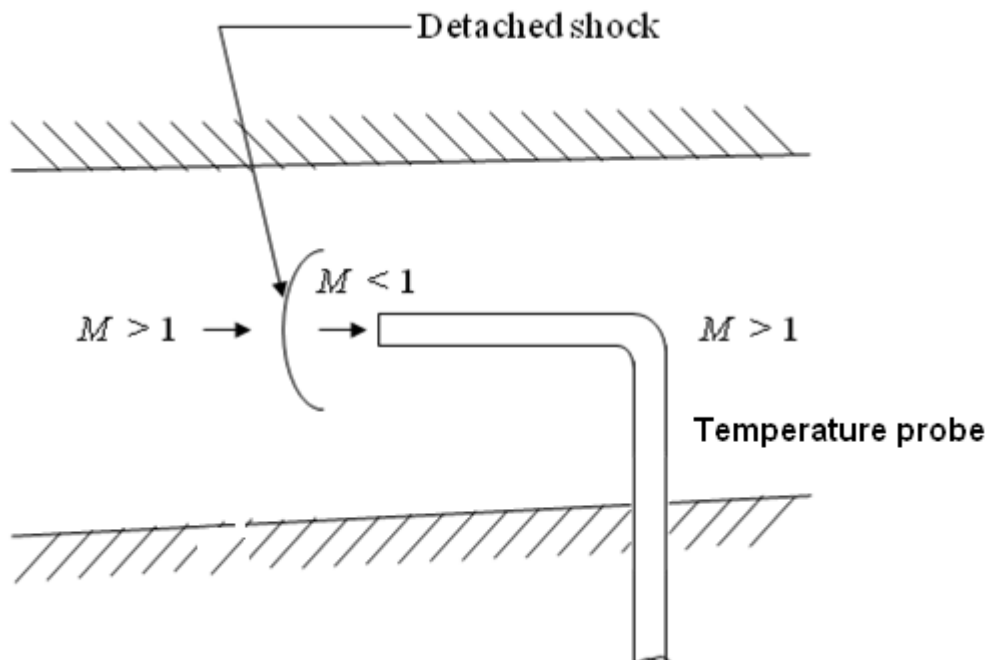


Fig. 7.5.3: Detached shock ahead of the measuring temperature probe in a supersonic flow.

## Module 7 : Lecture 6

### MEASUREMENTS IN FLUID MECHANICS (Compressible Flow – Part II)

#### Measurement of Pressure

Many pressure measuring devices used for incompressible flows can be equally applicable for compressible flows if they are feasible for measurements in gases. They may be grouped into manometers and pressure transducers depending on the ranges of pressure and degree of precision. U-type liquid manometer, dial-type pressure gauge (Bourdon tube), electrical/mechanical/optical types of pressure transducers are few popular pressure measuring devices.

With respect to compressible flow field, the measurement concept of both *static* and *stagnation pressure* (Fig. 7.6.1) are equally important. Both the pressures along with the temperature can be used for calculating local flow velocity, Mach number and density of the flowing stream. When the measurement is made in such a way that the velocity of the flow is not disturbed, then the measured pressure indicates the *static pressure*. On the other hand, if the flow is brought to rest isentropically, then the pressure obtained, becomes the *stagnation pressure*.

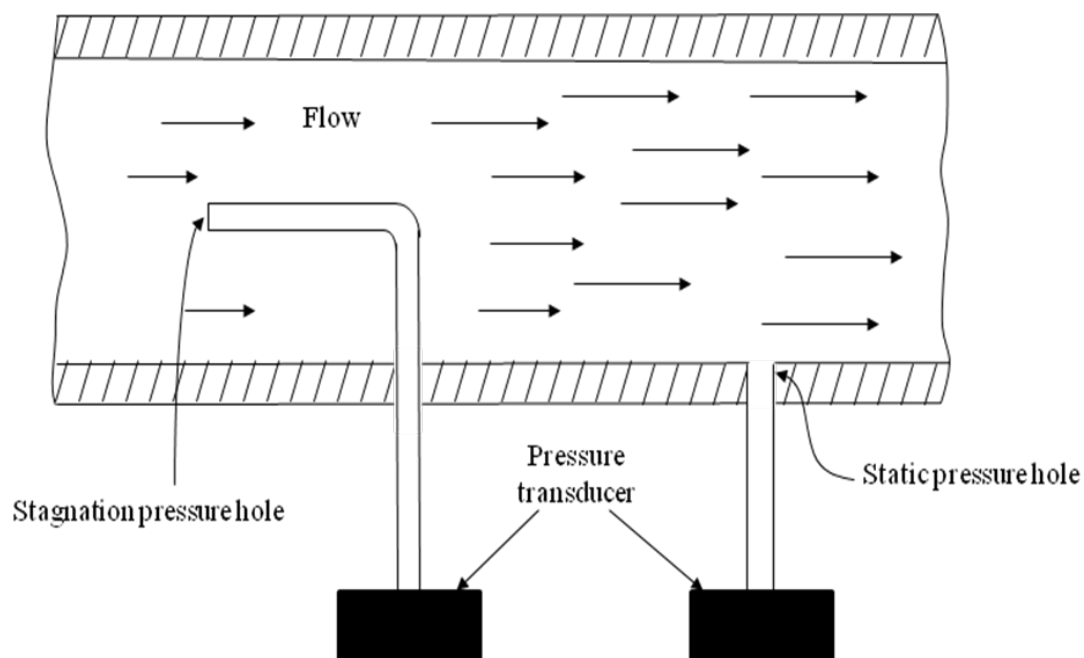


Fig. 7.6.1: Measurement concepts of static and stagnation pressures.



**Static Pressure Measurement:** The wall static pressure measurement is important in situations like inner walls of duct flows, surface of an airfoil etc. Here, a small hole is drilled normal to the surface (commonly called as pressure tapping) so that pressure measuring device can be connected (Fig. 7.6.2-a). In order to measure the static pressure at any interior point in the flow, a probe may be inserted without disturbing the flow streamlines (Fig. 7.6.2-b). The static pressure of the fluid stream over the surface is transmitted through orifice in the plane of the flow and subsequently recorded by the pressure measuring instrument. While measuring pressures through probe, the position of sensing holes and the support stem is very important. The deviation of actual and measured pressure may arise due to nose effect and stem effect. Since, both the effects have opposite nature; it may be possible to cancel these effects by suitable design.

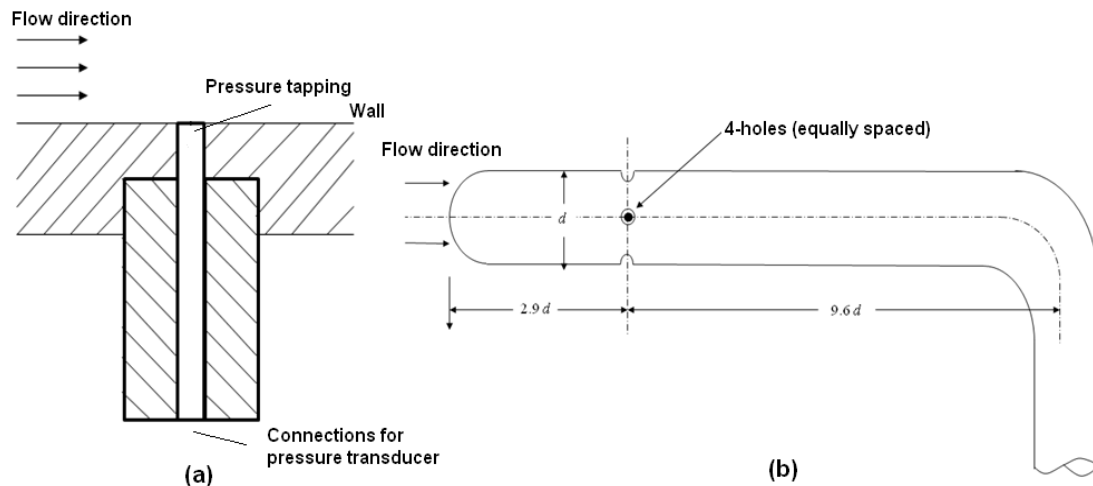


Fig. 7.6.2: Static pressure measurements in compressible flows: (a) wall pressure tapping; (b) static pressure probe.

**Stagnation Pressure Measurement:** The stagnation pressure is an indication of entropy level in a flowing fluid and the change in entropy is associated to the irreversibility. When the flow from a reservoir takes place isentropically, the static pressure record of the fluid in the reservoir indicates the stagnation pressure of the fluid. This situation of measuring pressure is analogous when the flowing stream is brought to rest isentropically. However, due to many irreversibility associated to the flow such as shock wave and frictional effects, the stagnation pressure may not be equal to the reservoir pressure. So, this pressure is always measured locally in the flow field. In order to measure the stagnation pressure at any local section, a stagnation probe is placed in the stream parallel to the flow with its open end facing the flow as shown in Fig. 7.6.3. Thus, it allows the fluid to get decelerated

isentropically to rest through the passage. The reading in the probe gives the stagnation pressure at the location where the nose of the probe is oriented. This device was first used by Henery Pitot for measurement of pressure and hence named as *Pitot tube*. At low Reynolds number flow, the deceleration may not be isentropic and inaccuracy in the measurements can arise.

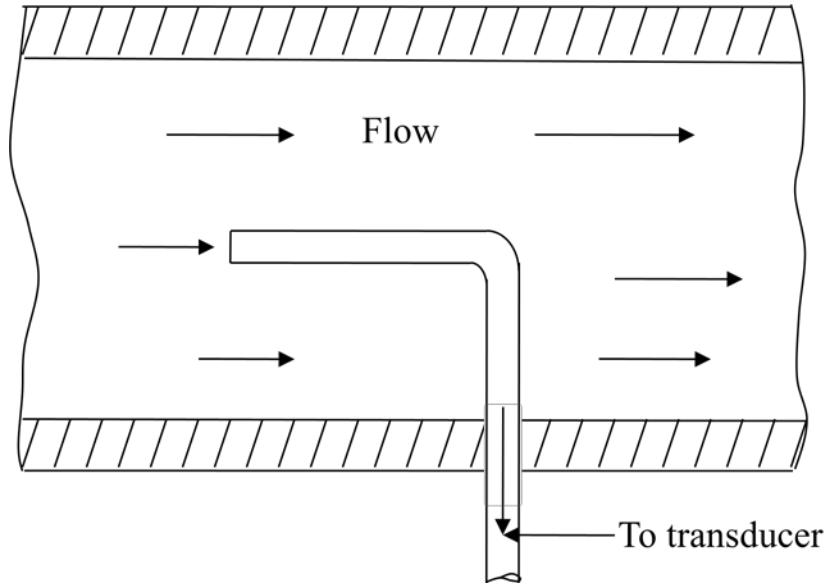


Fig. 7.6.3: Pitot tube for stagnation pressure measurement.

### Measurements of Flow Velocity

In most of the cases, the flow velocity is obtained through simultaneous measurement of static and stagnation pressures using a *Prandtl Pitot Static probe* (Fig. 7.6.4). It has opening at the nose for stagnation pressure communications while several number of equal size holes are made around the circumference of the probe at the location downstream of the nose. The difference pressure gives the dynamic pressure. Further, Bernoulli equation can be applied to calculate the flow velocity.

$$\frac{dp}{\rho} + VdV + gdz = 0 \quad \Rightarrow \quad \int \frac{dp}{\rho} + \frac{V^2}{2} + gz = \text{constant} \quad (7.6.1)$$

Now, replace the integral of Eq. (7.6.1) with the isentropic relation for gases;

$$p = c \rho^\gamma \quad \Rightarrow \quad \frac{dp}{\rho} = c^\gamma \rho^{\gamma-2} d\rho \quad (7.6.2)$$

where,  $p$ ,  $\rho$  and  $V$  are the pressure, density and velocity, respectively,  $z$  is the elevation difference,  $\gamma$  is the specific heat ratio and  $c$  is a constant. Combine Eq.

(7.6.1 & 7.6.2) and simplify to obtain the Bernoulli equation for one-dimensional frictionless isentropic flow for compressible fluid.

$$\frac{\gamma}{\gamma-1} \frac{p}{\rho} + \frac{V^2}{2} + gz = \text{constant} \quad (7.6.3)$$

Apply Eq. (7.6.3) along a stream line at the location of stagnation point and any desired location to obtain the flow velocity.

$$\frac{\gamma}{\gamma-1} \frac{p}{\rho} + \frac{V_\infty^2}{2} = \frac{\gamma}{\gamma-1} \frac{p_0}{\rho_0} \Rightarrow V_\infty = \left[ \frac{2\gamma}{\gamma-1} \left( \frac{p_0}{\rho_0} - \frac{p}{\rho} \right) \right]^{\frac{1}{2}} \quad (7.6.4)$$

The subscripts, 0 and  $\infty$  refers to stagnation and free stream conditions, respectively. Had the flow been incompressible, the density term in Eq. (7.6.1) becomes constant quantity and the stagnation and static pressure difference is expressed as follows:

$$p_0 - p = \frac{1}{2} \rho V_\infty^2 \Rightarrow V_\infty = \sqrt{\frac{2(p_0 - p)}{\rho}} \quad (7.6.5)$$

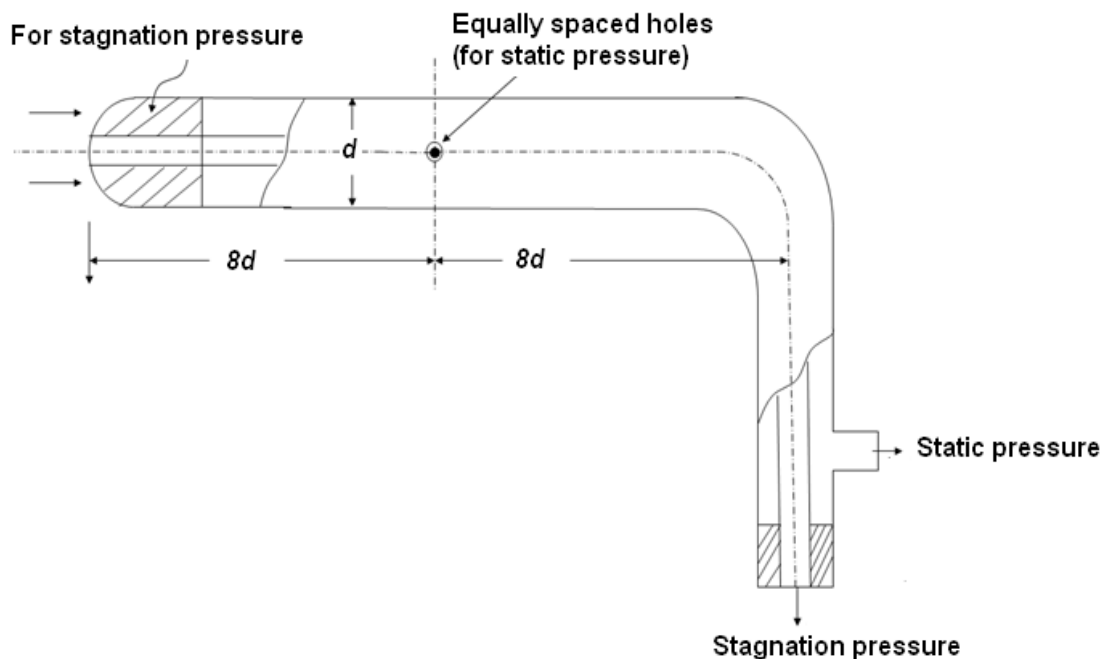


Fig. 7.6.4: Prandtl Pitot static probe for simultaneous measurement.

## Measurements for Subsonic and Supersonic Flows

The flow Mach number is one of the important parameter for subsonic and supersonic flows. All the flow parameters and their variations are the functions of local Mach number ( $M$ ). The pressure measurements are one of the common practices to determine the Mach number. In subsonic flow, the simultaneous measurement of static ( $p$ ) and stagnation pressures ( $p_0$ ) using a *Prandtl Pitot Static tube* are made in a similar way as shown in Fig. 7.6.4. Subsequently, the isentropic relation is used to determine the flow Mach number.

$$\frac{p_0}{p_\infty} = \left( 1 + \frac{\gamma-1}{2} M_\infty^2 \right)^{\frac{\gamma}{\gamma-1}} \quad (7.6.6)$$

The characteristic feature of a supersonic flow is the formation of a shock wave. So, the introduction of a *Pitot probe* into the flow stream, leads to a detached bow shock (Fig. 7.6.5). Due to this shock wave at certain distance from the measurement location, the stagnation pressure located indicated by the probe will be much higher than the stagnation pressure of the free stream. For the stagnation stream lines, the curved shock is normal to the free stream and the measured value represents the stagnation pressure downstream of the normal shock ( $p_{02}$ ). While conducting experiment, the static pressure ( $p_\infty$ ) of the free stream (upstream of the shock) is also measured simultaneously by any of the methods, discussed in Fig. 7.6.2. However, the static pressure measurement must be done far upstream of the shock so that its influence on the measurement will be minimized. The Mach number relation connecting the static and stagnation pressure measurements is expressed by *Rayleigh-Pitot* formula for supersonic flows.

$$\frac{p_{02}}{p_\infty} = \frac{\left( \frac{\gamma-1}{2} M_\infty^2 \right)^{\frac{\gamma}{\gamma-1}}}{\left( \frac{2\gamma}{\gamma+1} M_\infty^2 - \frac{\gamma-1}{\gamma+1} \right)^{\frac{1}{\gamma-1}}} \quad (7.6.7)$$

The *Rayleigh-Pitot formula* with air as free stream is presented graphically in Fig. 7.6.6. The dynamic pressure ( $p_d$ ) obtained from static pressure and the Mach number is then given by the following expression.

$$\frac{p_d}{p_\infty} = \frac{\gamma M_\infty^2}{2} \quad (7.6.8)$$

Thus, the Mach number calculation through static and stagnation measurements gives complete information of a supersonic flow field.

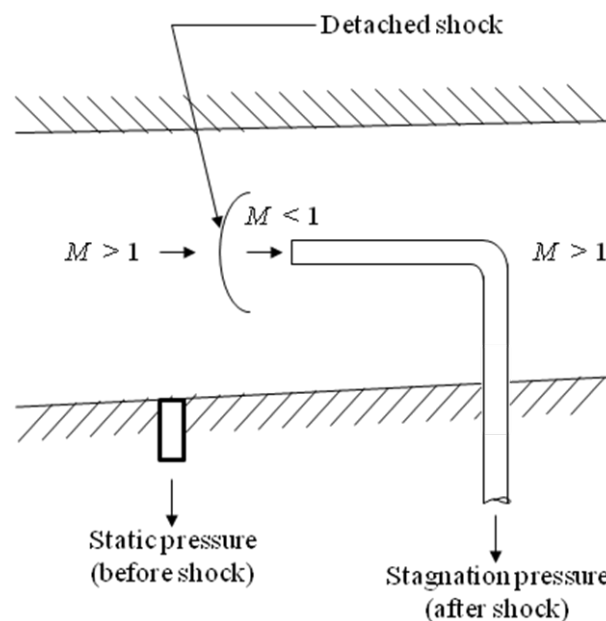


Fig. 7.6.5: Detached shock ahead of the measuring pressure probe in a supersonic flow.

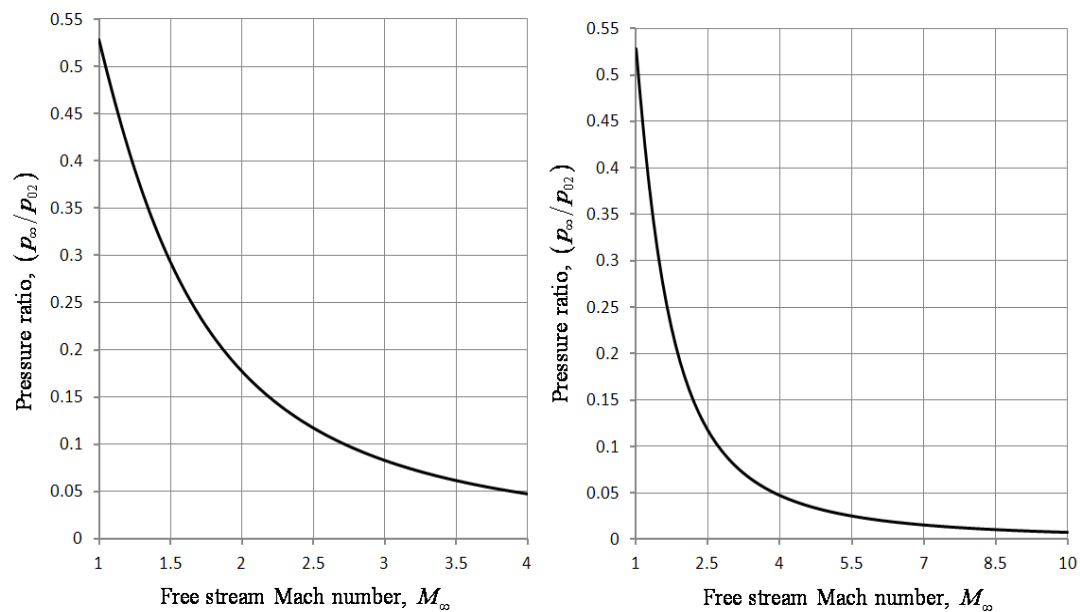


Fig. 7.6.6: Mach number determination from Pitot tube measurement in a supersonic flow.

Sonic Nozzle: It is an obstruction device often used to measure high flow rates for gases. When the flow rate is sufficiently high, the pressure differential is also expected to be large. Under this condition, a sonic flow condition is achieved at the minimum flow area and the flow is said to be *choked*. Such a device is known as *sonic nozzle*. In this case, the flow rate takes the maximum value for a given inlet condition. If this inlet refers to a reservoir pressure ( $p_0$ ), temperature ( $T_0$ ) and the flow is said to be choked at certain area ( $A^*$ ), then the pressure at this location ( $p^*$ ) can be obtained from isentropic relation,

$$\frac{p^*}{p_0} = \left( \frac{2}{\gamma + 1} \right)^{\frac{\gamma}{\gamma - 1}} \quad (7.6.9)$$

This relation is known as *critical pressure ratio for a choked nozzle*. The choked mass flow rate can be obtained by the following expression,

$$\dot{m}^* = \frac{p_0 A^*}{\sqrt{T_0}} \sqrt{\frac{\gamma}{R} \left( \frac{2}{\gamma + 1} \right)^{\frac{\gamma + 1}{\gamma - 1}}} \quad (7.6.10)$$

By designing the geometric parameter of a sonic nozzle, it is possible to achieve the discharge coefficient up to 0.97 corresponding to theoretical expression of flow rate given by the Eq (7.6.10).

## Module 7 : Lecture 7

### MEASUREMENTS IN FLUID MECHANICS (Compressible Flow – Part III)

#### Density Variation Techniques

The density of a flow can be calculated by measuring/determining the pressure and/or temperature. In the case of liquids, the density decreases slightly with temperature and moderately with pressure. All the gases at high temperatures and low pressures are in good agreement with the perfect gas law. So, for liquids, one can neglect the temperature effect and an empirical relation may be written for pressure ( $p$ ) and density ( $\rho$ ) while perfect gas equation can be stated ideal gases as given below;

$$\text{Liquids: } \frac{p}{p_a} \approx (B+1) \left( \frac{\rho}{\rho_a} \right)^m - B \quad (7.7.1)$$

$$\text{Gases: } p = \rho RT$$

where,  $p_a$  and  $\rho_a$  are the standard atmospheric value,  $B$  and  $m$  are the dimensionless parameters. For example, water can be approximately fitted to Eq. (7.7.1) with  $B \approx 3000$  and  $m \approx 7$ . Since the liquids are generally treated incompressible, the density variation is neglected. But, for compressible flows, the variation in density can be considered as an important tool to investigate the flow patterns during the experiments. The general principle for flow visualization for incompressible flow is to render the fluid elements visible either by observing the motion of suitable foreign materials added to the fluid. The other way is to use optical pattern resulting from variation in optical properties of the fluid such as refractive index. This technique is applicable for studying the flow pattern in compressible flows. In high-speed flows, the density changes are adequate to make these phenomena sufficient for optical observation.

### Principle of optical instruments

There are three types of optical instruments, generally used to study the flow pattern using the concept of density variation. They are *interferometer*, *Schlieren apparatus* and *shadowgraph*. All the three instruments have the following common characteristic phenomena.

- Variation in density of a gas stream produces a corresponding change in the refractive index of the gas.
- Light passing through a gaseous stream with density gradient gets deflected in the same manner as it does through a prism.

The refractive index in the medium of the flow field and the velocity of light through the flow field are functions of the fluid density in the flow field. Since the refractive index for most of the gases is close to unity, the relationship between the refractive index ( $n$ ) and the density of the gas medium ( $\rho$ ) is obtained through *Gadsone-Dale* equation.

$$\frac{n-1}{\rho} = \frac{n_1-1}{\rho_1} = \frac{n_2-1}{\rho_2} = \text{constant} \quad (7.7.2)$$

or,  $n = 1 + K_c \rho$

Here, the subscripts '1' and '2' denote two different conditions of the medium and the constant ( $K_c$ ) is different for if the gaseous medium is changed. Eq. (7.7.2) is applicable for most of the gases except for very dense gases. Since, the fluid density varies with location and time, the refractive index also follows the similar variation.

Let us consider a light ray passing through a compressible flow system enclosed in a glass walls (Fig. 7.7.1). If the region inside the wall is same as outside, then the light ray will follow a straight path and strike at a point  $S_1$  on the screen. If the medium inside the glass wall has different density, the refractive index will change and the light ray will get deflected through an angle ( $d\theta$ ), striking at some other point  $S_2$  (at a distance  $dz$  from  $S_1$ ). Also, there will be a time difference ( $dt$ ) due to the deflection of light ray, thereby covering more distance. Now, there are three measurable quantities ( $d\theta$ ,  $dz$  and  $dt$ ) due to density variation in the medium enclosed by glass wall and the medium outside. The operating principle of optical instruments is based on these measured quantities. Depending on the arrangements of the basic systems and optics used for observation of density variation, it is possible to



get the indication of variation in density, density gradient (first derivative of density) and change in density gradient (second derivative of density) as shown in Figs 7.7.2(a-c). In a typical flow field, an interferometer is useful in getting the density change directly by measuring  $dt$ , the *Schlieren apparatus* is useful in studying the density gradient from the information of  $d\theta$  and the shadowgraph gives an indication of change in density gradient by measuring  $dz$ .

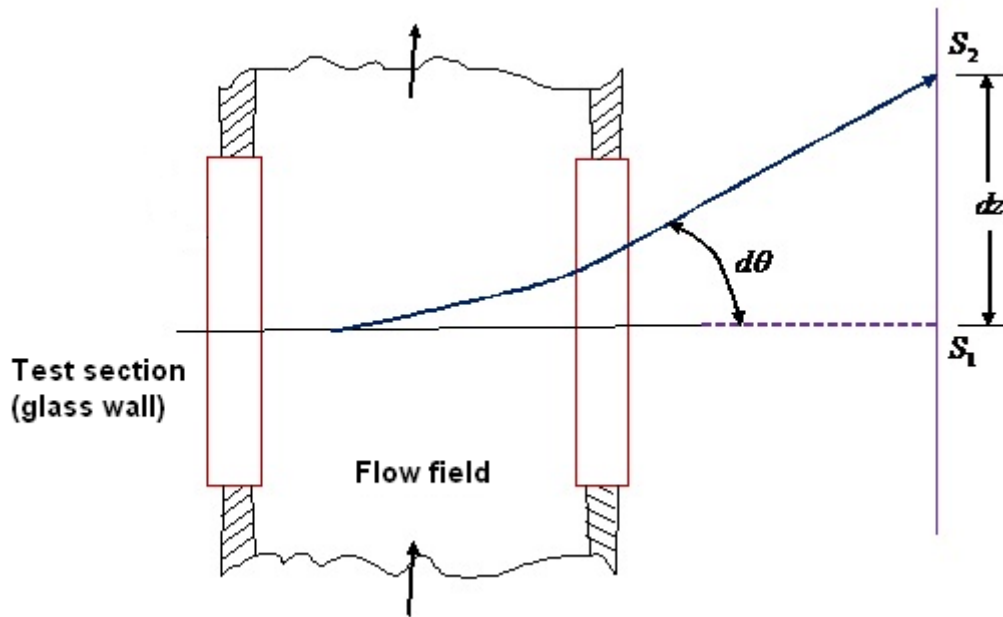


Fig. 7.7.1: Deflection of light ray in a flow field.

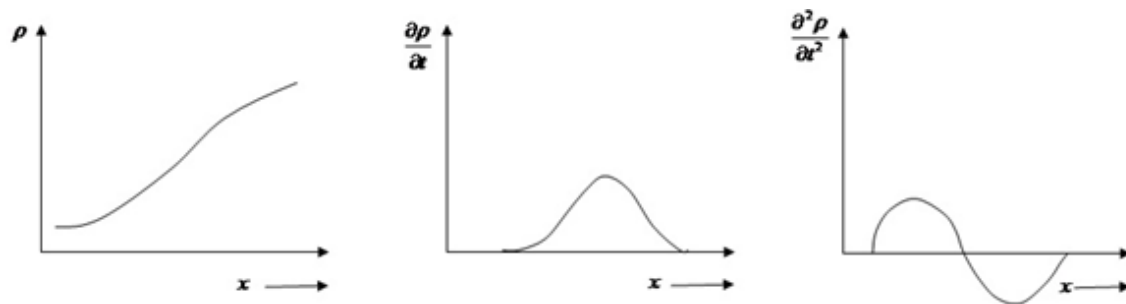


Fig. 7.7.2: Density variations in a flow field.

**Schlieren Apparatus:** Consider two parallel beam of light passing through a test section at same initial condition (Fig. 7.7.3). The test section is divided into two parts  $T_1$  and  $T_2$  and a lens with focal length  $f$  is placed at a distance  $l$  from the test section. A knife edge is kept at the focal point so that it can be moved up/down, thus creating an obstruction to the light ray. A screen is placed at some appropriate location such that the light rays passing through the test section can illuminate the screen bright/dark depending on the position of the knife edge. It is also possible to

divide the screen into two parts  $S_1$  and  $S_2$  such that  $S_1$  is the image of  $T_1$  and  $S_2$  is the image of  $T_2$ . If two regions of the test section of the fluid are same, then the images will also be the same. When the density of the gas in  $T_2$  change by keeping  $T_1$  as the same, the light rays passing through  $T_2$  will be show dark/bright image  $S_2$  in the screen depending on the decrease/increase in the density of the medium. In other words, if a disturbance is introduced in the test section, the light will be refracted so that the image is displaced by a distance  $dz$ . Thus, the illumination on the screen is proportional to  $dz$  which becomes the measure of density gradient of the flow. For most of the gases, the refractive index is close to unity and the deflection is small. Using electromagnetic theory, *Schlieren equation* is used to obtain the deflection angle ( $\theta_z$ ) in the  $z$ -direction.

$$\theta_z = \frac{\partial n}{\partial z} dx = \frac{3r_s}{2} \frac{\partial \rho}{\partial z} dx, \text{ where } r_s \text{ is the specific refraction.} \quad (7.7.3)$$

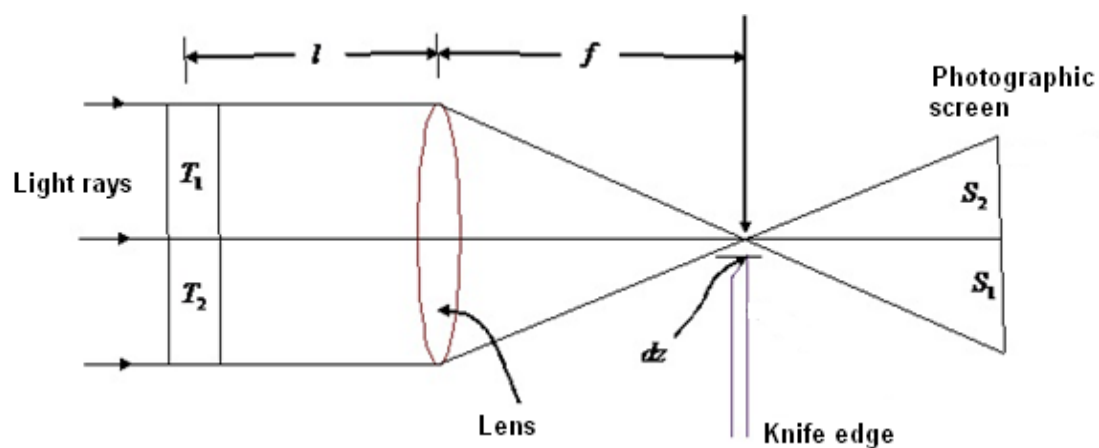


Fig. 7.7.3: Principle of a Schlieren system.

The basic components of a widely used *Toepler-Schlieren* arrangement are shown in Fig. 7.4.4. The system consists of a point light source (typically mercury lamp), a condensing lens, a slit, two identical lenses, a knife edge and a screen. The condensing lens increases the effective size of the source and the slit controls the light passing through the first lens to beams that parallel to the test section. The parallel beams get focused at the knife edge with the help of second lens. Finally, the image is produced on the screen. Many a times, it is difficult to obtain high quality lenses of large sizes. So, parabolic mirrors may be employed to get parallel beams. It may be noted that the positions of image points on the viewing screen are not affected by the deflection of light rays in the test section. Since, the deflected rays are again brought to focus in the focal plane and the screen is uniformly illuminated when the knife edge is not inserted into the light beam.

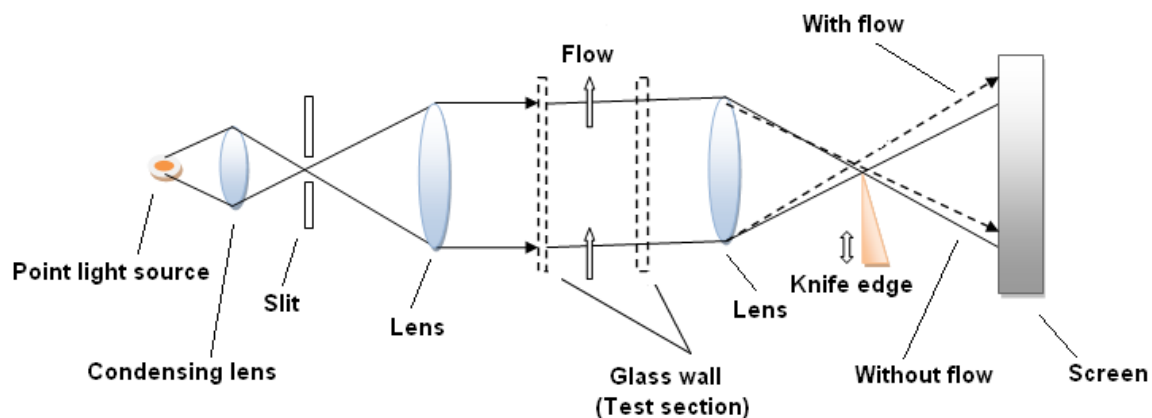


Fig. 7.4.4: Schematic arrangement of a *Toepler-Schlieren* system.

A *Schlieren* system gives the deflection angles of incident rays and is very sensitive first derivative of density. Moreover, this system is preferable when the refractive index varies gradually. It is mainly used to study high-speed flows in the transonic and supersonic Mach number ranges and gives only a qualitative estimate of density gradients in the flow field. The applications include studies of shock and expansion waves, mixing, combustion, ignition and boundary layer studies.

**Shadowgraph:** The displacement experienced by an incident ray which has crossed the high speed flowing gas, is obtained through *shadowgraph technique*. In certain applications, like strong shock waves (hypersonic flows) and combustion phenomena, the density varies rapidly leading to sudden change in the refractive index. So, the second derivative of density can provide more information on the changes in the flow field than *Schlieren technique*.

A shadowgraph consists of a light source, a collimating lens and a viewing screen as shown in Fig. 7.4.5. Initially, let us assume stagnant air in the test section and the illumination on the screen of uniform intensity. When, the flow takes place through the test section, the light beam will be refracted wherever there is a density gradient. These rays will have a tendency to converge/diverge and the variations in illumination of the picture (intensity  $I$ ) on the screen are proportional to the second derivative of density.

$$\Delta I = k_c \left( \frac{\partial^2 \rho}{\partial x^2} + \frac{\partial^2 \rho}{\partial y^2} \right) \quad (7.7.4)$$

where,  $x$  and  $y$  are the coordinates in a plane normal to the light path and  $k_c$  is a constant. The intensity of illumination on the screen depends on the relative deflection of light rays ( $dz$ ) which is proportional to the change in the density gradient. On the screen, there are bright regions where the rays crowd together, dark regions represent the rays diverging and uniformity in the image shows that the brightness is average (Fig. 7.4.6).

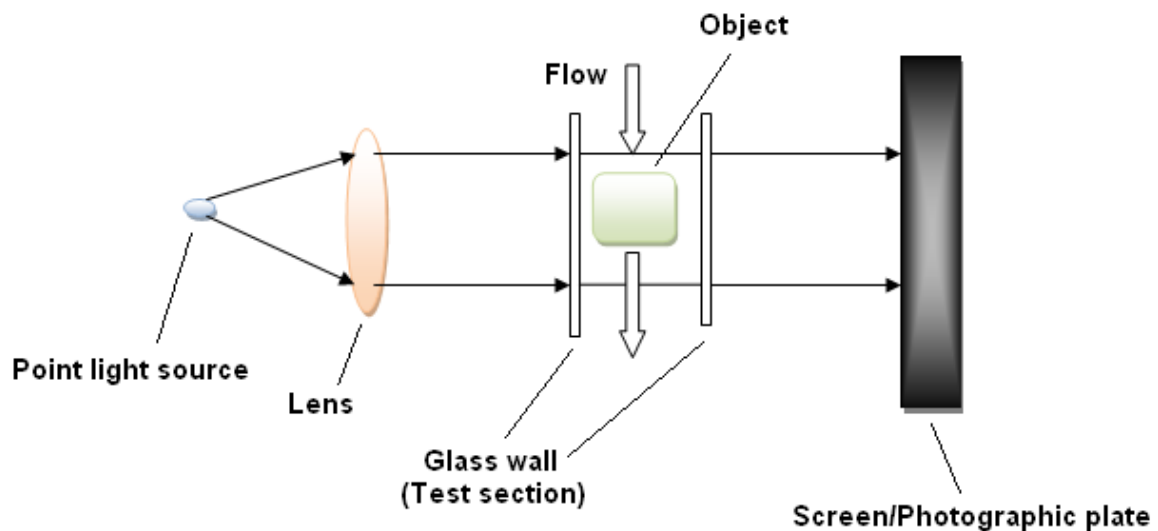


Fig. 7.4.5: Schematic arrangement of a *shadowgraph* system.

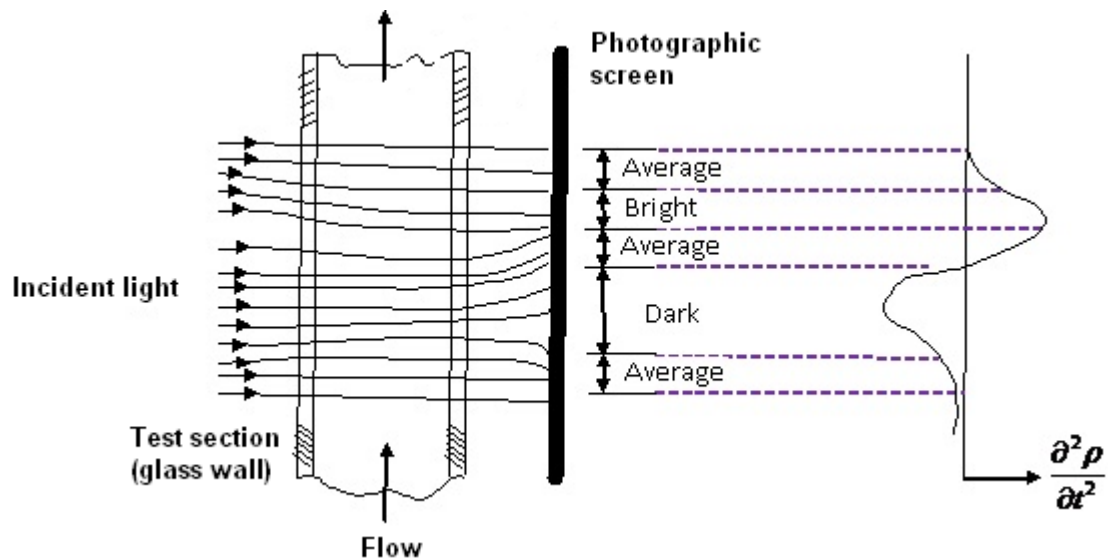


Fig. 7.4.6: Intensity of illumination with respect to variation of density gradient.

In contrast to *Schlieren apparatus*, the screen can be placed close to the test section so that the deflection of light is visible and this phenomenon is known as *shadow effect*. Also, the point source of light is sufficient and there is no need of lenses to split the light source. Moreover, the rays need not be parallel when it enters the test section. This simplicity makes the shadowgraph less expensive compared to *Schlieren apparatus* and often used when the fine details of density information are not required.

Interferometer: The optical phase changes resulting from relative retardation of disturbed rays in a flow field can provide qualitative estimate of flow density by using the instrument interferometer. It works on the principle of interference as shown in Fig. 7.4.7.

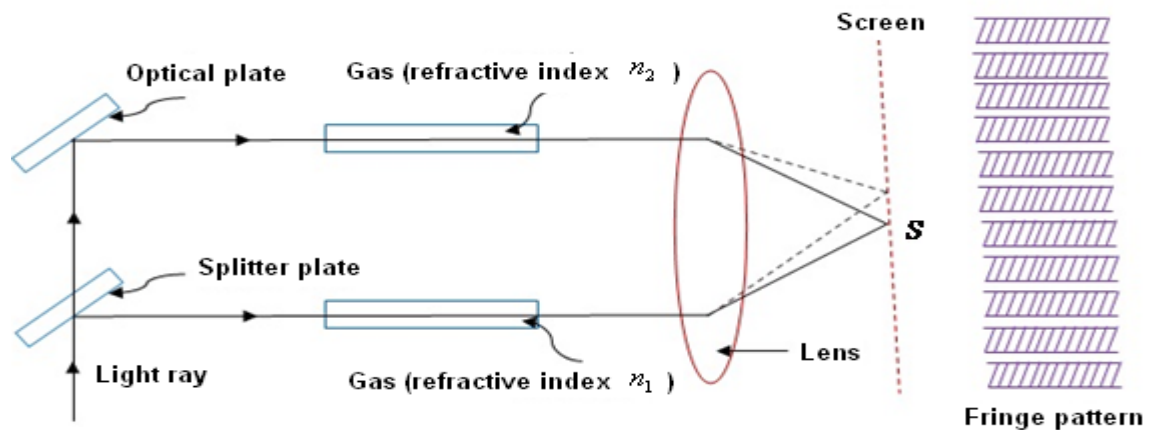


Fig. 7.4.7: Operating principle of an interferometer.

Consider two rays from same source arrive at a point  $S$  on the screen through different paths. Depending on the length of the paths, the rays will have a phase difference and they will interfere when brought together. Due to the interference between the rays, *fringes* are formed in the screen with alternate bright and dark regions. The number of fringes generated, depends on the difference in path lengths of the two beams. If the two rays pass through identical gas medium, then the path difference is due to geometrical arrangements of the mirrors that can be adjusted to get a set of fringes on the screen. When one of the rays passes through a different gas, the refractive index of the medium will change. So, the fringes will differ by an amount  $N\lambda$ , where  $\lambda$  is the wavelength of light and  $N$  is an integer. Hence, the order of interference at the point  $S$  is changed by amount  $N$  (i.e. shift of  $N$  fringes). The shift in fringes can be recorded by taking the photographs with/without the flow. It is then correlated to equivalent change in the optical path and subsequently to the change in the density.

Initially, let us take the refractive index of both the rays as  $n_1$ . When the second ray passes through different gas, its refractive index increases to  $n_2$  because the speed of the light decreases from  $C_0/n_1$  to  $C_0/n_2$ . So, the additional time ( $\Delta t$ ) required to travel certain length ( $L$ ) in the flow field is given as follows;

$$\Delta t = \frac{L}{C_0}(n_2 - n_1) \quad (7.7.5)$$

The corresponding change in the optical path ( $\Delta L$ ) can be correlated to density changes through Eq. (7.7.2).

$$\Delta L = C_0 \Delta t = L(n_2 - n_1) = K_c L(\rho_2 - \rho_1) \quad (7.7.6)$$

Thus, the number of fringe shift ( $N$ ) on the screen is obtained as,

$$N = \frac{K_c L}{\lambda}(\rho_2 - \rho_1) \quad (7.7.7)$$

There are different arrangements of interferometer to record fringe patterns directly and the most widely used one is the *Mach-Zehnder interferometer*. This arrangement has four optical plates (two reflecting mirrors  $M_1$  &  $M_2$  and two splitters  $S_1$  &  $S_2$ ) parallel to each other on the corners of a rectangle. The splitters are nothing but the silvered mirrors that reflect half of the incident light falling on it and transmit the remaining half while the mirrors completely reflect the rays falling on them. The monochromatic light from a source is converted into parallel beam of light by a concave mirror  $C_1$ . The splitter  $S_1$  divides the beams by partial reflection and transmission. The reflected part passes through the test flow domain, reflected completely by mirror  $M_2$ , passes through  $S_2$  and subsequently reaches the concave mirror  $C_2$ . Similarly, the other transmission part of the beam is reflected completely through  $M_1$ , passes through the reference section and reaches to the concave mirror  $C_2$  through  $S_2$ . This concave mirror  $C_2$  collects the rays separately coming from the reference section and test domain. Subsequently, the rays are directed on the screen/photographic plate and an image is obtained through formation of fringes. The number of fringes (i.e. difference in the wavelength in the path) indicates the density difference between the test medium and reference section.

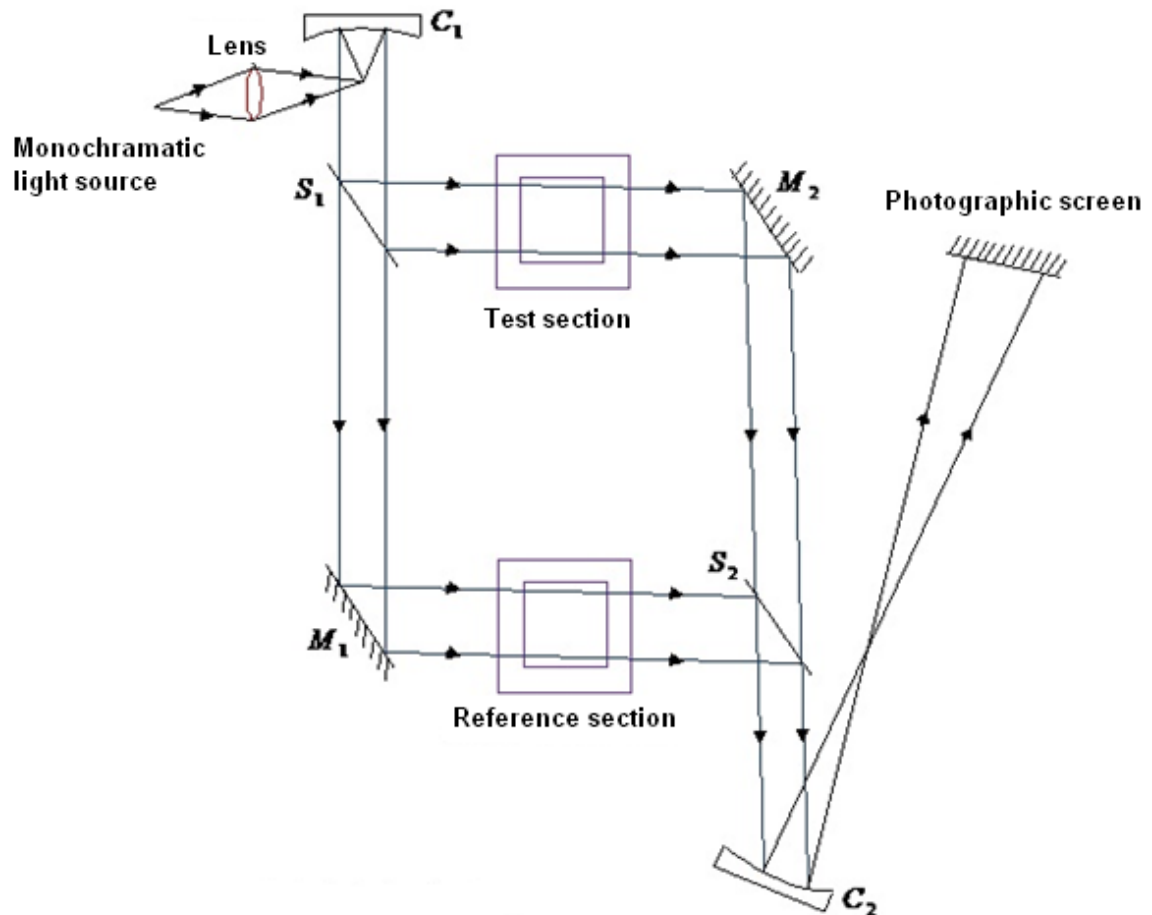


Fig. 7.4.8: Schematic representation of a *Mach-Zehnder* interferometer.

In the previous techniques (*Schlieren/Shadowgraph*), the image of the flow field depends on the first and second derivative of the density. Subsequently, the density field may be obtained by integration. Interferometer works on the principle of interference and is used to obtain the density information directly in the flow field. They are widely used to visualize high speed flows in the transonic/supersonic Mach number ranges. Even though, it is suitable for quantitative determination of density, its usages are limited due to expensive equipments involved.